

Pre-thermalized Gravitational Waves

Nicolás Bernal ^a, Quan-feng Wu ^b, Xun-Jie Xu ^b and Yong Xu ^c

^a*New York University Abu Dhabi*

PO Box 129188, Saadiyat Island, Abu Dhabi, United Arab Emirates

^b*Institute of High Energy Physics, Chinese Academy of Sciences, Beijing 100049, China*

^c*PRISMA⁺ Cluster of Excellence and Mainz Institute for Theoretical Physics
Johannes Gutenberg University, 55099 Mainz, Germany*

E-mail: nicolas.bernal@nyu.edu, wuquanfeng@ihep.ac.cn,
xuxj@ihep.ac.cn, yonxu@uni-mainz.de

ABSTRACT: We investigate a novel gravitational wave (GW) production mechanism from gravitons generated during the pre-thermal phase of cosmic reheating, where the energy density is dominated by non-thermalized inflaton decay products, dubbed *reheatons*. We consider multiple production channels, including: *i*) pure inflaton-inflaton annihilation, *ii*) graviton Bremsstrahlung from inflaton decay, *iii*) scatterings between an inflaton and a reheaton, and *iv*) scatterings among reheatons. To determine the resulting GW spectrum, we solve the Boltzmann equation to obtain the graviton phase-space distribution for each channel. We find that the third channel, *iii*), dominates due to the large occupation number of reheatons at highly-energetic states during the pre-thermalization phase. Notably, in scenarios with a low inflaton mass, the GW spectrum could fall within the sensitivity range of future experiments such as the Einstein Telescope, the Cosmic Explorer, the Big Bang Observer, and ultimate DECIGO.

Contents

1	Introduction	1
2	The Model	3
3	Pre-thermalization and thermalization	4
3.1	Inflatons after Inflation	4
3.2	Non-thermal Reheatons	6
3.3	Standard Model Thermal Bath	7
4	Gravitational Waves	8
4.1	$\phi\phi \rightarrow hh$	11
4.2	$\phi \rightarrow \varphi\varphi h$	13
4.3	$\phi\varphi \rightarrow \varphi h$	13
4.4	$\varphi\varphi \rightarrow hh$	14
4.5	Comparison	15
5	Conclusions	17
A	Calculation of $\mathcal{M} ^2$	18
A.1	Gravitational Polarization Summation	18
A.2	Graviton Production from Scalar Annihilation	19
A.3	Graviton Production from Bremsstrahlung	21
A.4	Graviton Production from Inflaton and Reheaton Scattering	22
B	Collision Terms Γ_h	23
B.1	$\phi \rightarrow \varphi\varphi h$	23
B.2	$\phi\varphi \rightarrow \varphi h$	24
C	Comparing Analytical with Numerical Results	24

1 Introduction

The early Universe hosts a variety of gravitational wave (GW) sources. In inflationary cosmology, the tensor perturbations generated during cosmic inflation provide one such source [1]. Following inflation, the energy stored in the inflaton field must be transferred to other fields to reheat the Universe and establish a thermal radiation-dominated epoch with a temperature of at least $\mathcal{O}(\text{MeV})$ to ensure a successful Big Bang Nucleosynthesis (BBN) [2–5]. This energy transfer process, known as cosmic reheating [6–8], can itself be a source of GWs, depending on the specific setup of the reheating model and the

relevant dynamics involved. In addition, GWs can be produced through non-perturbative preheating effects [1].

In this work, we focus on GW production in the context of perturbative reheating. In this regard, several mechanisms have been explored in the literature, including *i*) non-thermal graviton production processes such as graviton Bremsstrahlung [9–20] and graviton pair production from inflaton annihilation [21–24], *ii*) graviton production from inflaton scattering with thermalized daughter particles [25], and *iii*) graviton production from the scattering between thermalized daughter particles during reheating [26]. We also refer to Refs. [27–35] for studies of GW production from thermal plasma interactions in the radiation-dominated epoch after reheating. Previous studies such as Refs. [25, 26] have assumed daughter fields that feature sizable gauge couplings with fast and instantaneous thermalization during reheating.

In contrast to these earlier works, we investigate for the first time a novel GW production channel where gravitons are emitted during the *pre-thermal phase* of reheating. To this end, we assume the inflaton decay products to have small self-interactions, and to feebly communicate with the standard model (SM) particle content. Consequently, a slow thermalization is expected. This phase is particularly interesting because of the presence of numerous non-thermalized hard daughter particles with momenta of order of the inflaton mass. Since graviton production is an ultraviolet (UV) dominated process,¹ the production rate is expected to be higher than that from scatterings involving thermalized particles. Consequently, we anticipate an enhancement of the GW spectrum arising from this early phase, which we refer to as pre-thermalized GWs.² This constitutes the primary objective of the present study.

Furthermore, we apply a systematic approach to study the GW spectrum by solving the Boltzmann equation at the phase-space distribution level, offering a robust cross-check with existing methods and results in the literature. This serves as another key objective of our work. Interestingly, the produced GW spectra turn out to be within the reach of next-generation GW observatories. In addition, since GWs propagate as dark radiation, they contribute to the effective number of neutrino species, N_{eff} . This contribution is also taken into account in the analysis.

The remainder of this article is structured as follows. In Section 2, we introduce the model setup. Section 3 discusses the pre-thermal and thermal phases of reheating. In Section 4, we present the GW spectra, with particular emphasis on those produced during pre-thermalization, and provide a comparison with other sources. Finally, we summarize our main findings in Section 5. Appendices A and B contain detailed computations of matrix elements and collision terms relevant to graviton production. The analytical derivation and the comparison with fully numerical results for the GW spectrum are presented in Appendix C.

¹This is analogous to the UV freeze-in mechanism for dark matter production during pre-thermalization [36].

²Note that here we specifically refer to GWs produced during the pre-thermalization phase. Moreover, the temperatures under consideration remain well below the Planck scale, ensuring that gravitons do not thermalize.

2 The Model

We consider a minimally coupled gravity framework, where the action is given by

$$S \supset \int d^4x \sqrt{-g} [\mathcal{L}_{\text{EH}} + \mathcal{L}_\phi + \mathcal{L}_{\phi\varphi} + \mathcal{L}_\varphi]. \quad (2.1)$$

Here, g denotes the determinant of the metric $g_{\mu\nu}$, $\mathcal{L}_{\text{EH}} = \frac{1}{2} M_P^2 R$ represents the Einstein-Hilbert term for gravity,³ and R is the Ricci scalar, and $M_P \equiv 1/\sqrt{8\pi G_N} \simeq 2.4 \times 10^{18}$ GeV is the reduced Planck mass. The second term in Eq. (2.1) corresponds to the Lagrangian density of a real singlet inflaton field ϕ , given by

$$\mathcal{L}_\phi = \frac{1}{2} g^{\mu\nu} \partial_\mu \phi \partial_\nu \phi - V(\phi), \quad (2.2)$$

where $V(\phi)$ represents the inflaton potential. Although this potential may have a complicated form during inflation, it is assumed to be approximated by $V(\phi) \simeq \frac{1}{2} m_\phi^2 \phi^2$ after inflation, particularly during the oscillatory phase of the inflaton. This quadratic form occurs in various inflationary models, including Starobinsky inflation [40], certain classes of α -attractor models [41, 42], and both small- and large-field polynomial inflation scenarios [43–46]. Depending on the specific inflationary model, the inflaton mass m_ϕ can vary significantly. For example, in the Starobinsky or large-field polynomial inflation model, it can be as large as $m_\phi \simeq 10^{13}$ GeV, whereas in a small-field polynomial inflationary scenario, it can be as low as $m_\phi \simeq 10^2$ GeV. In this work, we take an agnostic approach and treat the inflaton mass m_ϕ as a free parameter.

The third term in Eq. (2.1) describes the interaction between the inflaton and a real bosonic daughter field φ , which eventually mediates the energy transfer from the inflaton to the SM degrees of freedom; φ is therefore called the reheaton. We focus on inflaton decay via the interaction

$$\mathcal{L}_{\phi\varphi} \supset \frac{1}{2} \mu \phi \varphi^2, \quad (2.3)$$

where μ is a dimension-one coupling constant. This trilinear term induces an inflaton decay rate into a pair of reheatons

$$\Gamma_\phi = \frac{\mu^2}{32\pi m_\phi} \left[1 - \left(\frac{2m_\varphi}{m_\phi} \right)^2 \right]^{1/2} \simeq \frac{\mu^2}{32\pi m_\phi}, \quad (2.4)$$

where m_φ is the mass of φ .

The final term in Eq. (2.1) describes the free-field Lagrangian density for φ , given by

$$\mathcal{L}_\varphi = \frac{1}{2} g^{\mu\nu} \partial_\mu \varphi \partial_\nu \varphi - \frac{1}{2} m_\varphi^2 \varphi^2. \quad (2.5)$$

³In this paper, we adopt the $(+, -, -, -)$ sign convention for the metric. In addition, we should clarify that the Riemann and Einstein signs in our setup are $-$ and $+$, respectively. Hence, there is no extra minus sign in the Einstein-Hilbert term \mathcal{L}_{EH} . For further clarification, see the $(-, -, +)$ convention in the “table of sign conventions” of Ref. [37]. We have checked that the notation used in this work is the same as that in Refs. [38, 39].

Note that we have omitted any non-gravitational direct interactions between the inflaton and the SM degrees of freedom. Energy transfer to the SM sector occurs through the subsequent decays or annihilations of φ into SM degrees of freedom, which will be discussed in Section 3.3.

To derive the gravitational interaction vertex and the corresponding Feynman rules for graviton production, we expand the metric $g_{\mu\nu}$ around the Minkowski metric $\eta_{\mu\nu} = (+, -, -, -)$ as [38, 39]

$$g_{\mu\nu} = \eta_{\mu\nu} + \frac{2}{M_P} h_{\mu\nu}, \quad (2.6)$$

where $h_{\mu\nu}$ represents the massless spin-2 graviton field, which has mass dimension one. From Eq. (2.6), it follows that $\sqrt{-g} \simeq 1 + h/M_P$, where $h \equiv h^\mu_\mu$ denotes the trace of the graviton field; it is zero in the transverse and traceless gauge (TT). Substituting this expansion into the action, we obtain the effective interaction between the graviton and the energy-momentum tensor [38, 39]

$$\sqrt{-g} \mathcal{L} \supset -\frac{1}{M_P} h_{\mu\nu} \sum_k T_k^{\mu\nu}, \quad (2.7)$$

where $T_k^{\mu\nu}$ denotes the energy-momentum tensor of a given particle species k , including the inflaton, the reheaton, and the degrees of freedom in the SM. In particular, graviton production requires a non-zero anisotropic energy-momentum tensor, meaning that the spatial components must satisfy $T^{ij} \neq 0$ for $i, j = 1, 2, 3$. The energy-momentum tensor of the inflaton takes the form

$$T_\phi^{\mu\nu} = \partial^\mu \phi \partial^\nu \phi - \frac{1}{2} \eta^{\mu\nu} (\partial_\alpha \phi \partial^\alpha \phi - m_\phi^2 \phi^2), \quad (2.8)$$

which implies that $T_\phi^{ij} = 0$ due to the homogeneity of the inflaton condensate, leading to vanishing anisotropic components. Consequently, the amplitude for any Feynman diagram featuring an outgoing graviton directly coupled to an *on-shell* inflaton is zero [25].

3 Pre-thermalization and thermalization

3.1 Inflatons after Inflation

Just after the end of the cosmic inflationary era at a scale factor $a = a_I$, the Universe is dominated by non-relativistic inflatons ϕ of mass m_ϕ . Inflatons decay into pairs of ultra-relativistic reheatons φ with a total decay width Γ_ϕ given in Eq. (2.4). The evolution of the inflaton number density n_ϕ is given by

$$\frac{dn_\phi}{dt} + 3H n_\phi = -\Gamma_\phi n_\phi, \quad (3.1)$$

where H is the Hubble expansion rate, which implies that

$$n_\phi(t) = n_\phi(t_I) \left(\frac{a_I}{a(t)} \right)^3 e^{-\Gamma_\phi(t-t_I)}, \quad (3.2)$$

with a the cosmic scale factor, t_I and a_I correspond to the time and scale factor at the end of the inflationary era, respectively. The value of $n_\phi(t_I)$ can be extracted from the scale of inflation H_I :

$$n_\phi(t_I) = \frac{3 M_P^2 H_I^2}{m_\phi}. \quad (3.3)$$

It is interesting to note that, in a comoving frame, inflatons with momentum p_ϕ form a condensate characterized by a phase-space distribution

$$f_\phi(t, p_\phi) = (2\pi)^3 n_\phi(t) \delta^{(3)}(\vec{p}_\phi) = 2\pi^2 \frac{n_\phi(t)}{p_\phi^2} \delta(p_\phi). \quad (3.4)$$

Furthermore, taking into account that during this period the expansion of the Universe is dominated by non-relativistic inflatons,

$$H(a) = H_I \left(\frac{a_I}{a} \right)^{\frac{3}{2}}, \quad (3.5)$$

Eq. (3.2) can be expressed as

$$n_\phi(a) = \frac{3 M_P^2 H_I^2}{m_\phi} \left(\frac{a_I}{a} \right)^3 \exp \left[-\gamma_\phi \left(\frac{a}{a_I} \right)^{\frac{3}{2}} \left[1 - \left(\frac{a_I}{a} \right)^{\frac{3}{2}} \right] \right], \quad (3.6)$$

where the dimensionless parameter γ_ϕ is defined as

$$\gamma_\phi \equiv \frac{2}{3} \frac{\Gamma_\phi}{H_I}. \quad (3.7)$$

Given that for unitarity reasons $\mu \lesssim m_\phi$, it is expected that $\gamma_\phi \ll 1$. A small γ_ϕ also ensures that the inflaton decay becomes significant only after the end of the inflationary era and therefore has negligible effects on the slow-roll phase. Taking into account that in this era the Universe is dominated by non-relativistic inflatons, it follows that the evolution of the cosmic time is

$$t(a) = t_I + \frac{2}{3 H_I} \left[\left(\frac{a}{a_I} \right)^{3/2} - 1 \right]. \quad (3.8)$$

The period dominated by non-relativistic inflatons is followed by an era where ultra-relativistic reheats (i.e. radiation domination) drive the Hubble expansion of the Universe. The transition occurs at a scale factor $a = a_\phi$. Although it is not an instantaneous event, one can define it at the time $t = t_I + \Gamma_\phi^{-1}$, corresponding to

$$\frac{a_\phi}{a_I} = \left(\frac{1}{\gamma_\phi} + 1 \right)^{2/3} \simeq \gamma_\phi^{-\frac{2}{3}}. \quad (3.9)$$

From that moment on, ultra-relativistic reheats start to dominate the energy density of the Universe. Their phase-space distribution is explored in the next section.

3.2 Non-thermal Reheatons

At production, reheatoms are monochromatic with momentum $p_\varphi = m_\phi/2$. However, continuous production over time makes their distribution broad. The evolution of the phase-space distribution of the reheatoms can be followed by the use of the Boltzmann transport equation

$$\frac{\partial f_\varphi}{\partial t} - H p_\varphi \frac{\partial f_\varphi}{\partial p_\varphi} = \Gamma_\varphi, \quad (3.10)$$

where the collision term Γ_φ is

$$\begin{aligned} \Gamma_\varphi(t, p_\varphi) &= \frac{1}{2E_\varphi} \int d\Pi_{p_\phi} d\Pi_{p_{\varphi 2}} (2\pi)^4 \delta^{(4)}(p_\phi - p_\varphi - p_{\varphi 2}) |\mathcal{M}_{\phi \rightarrow \varphi\varphi}|^2 f_\phi(t, p_\phi) \\ &= 16\pi^2 \frac{n_\phi \Gamma_\phi}{m_\phi^2} \delta\left(p_\varphi - \frac{m_\phi}{2}\right) \end{aligned} \quad (3.11)$$

for ultra-relativistic reheatoms, with $d\Pi_i$ being the Lorentz-invariant phase space, E_φ the energy of the reheaton, and $|\mathcal{M}_{\phi \rightarrow \varphi\varphi}|^2 = \mu^2$ the squared amplitude for the decay $\phi \rightarrow \varphi\varphi$. Equation (3.10) can be analytically solved (see, e.g. Ref. [47]). The change of variable to the comoving momentum $\tilde{p}_\varphi \equiv a p_\varphi$ allows us to rewrite it as

$$\frac{df_\varphi(t, \tilde{p}_\varphi)}{dt} = \Gamma_\varphi, \quad (3.12)$$

which implies that

$$f_\varphi(t, \tilde{p}_\varphi) = 32\pi^2 \frac{\Gamma_\phi}{H(\tilde{a}')} \frac{n_\phi(\tilde{a}')}{m_\phi^3} \tilde{\Theta} \left[\frac{m_\phi}{2} a_I \leq \tilde{p}_\varphi \leq \frac{m_\phi}{2} a(t) \right] \quad (3.13)$$

for $\tilde{a}' \equiv 2\tilde{p}_\varphi/m_\phi$ and $\tilde{\Theta}$ the generalized Heaviside step function. In turn

$$f_\varphi(t, p_\varphi) = 32\pi^2 \frac{\Gamma_\phi}{H(a')} \frac{n_\phi(a')}{m_\phi^3} \tilde{\Theta} \left[\frac{m_\phi}{2} \frac{a_I}{a(t)} \leq p_\varphi \leq \frac{m_\phi}{2} \right] \quad (3.14)$$

for $a' \equiv 2p_\varphi a(t)/m_\phi$ which, in terms of the scale factor, becomes

$$\begin{aligned} f_\varphi(a, p_\varphi) &= 96\pi^2 \frac{M_P^2 H_I \Gamma_\phi}{m_\phi^4} \left(\frac{m_\phi}{2p_\varphi} \frac{a_I}{a} \right)^{\frac{3}{2}} \exp \left[\gamma_\phi \left(1 - \left(\frac{2p_\varphi}{m_\phi} \frac{a}{a_I} \right)^{\frac{3}{2}} \right) \right] \\ &\quad \times \tilde{\Theta} \left[\frac{m_\phi}{2} \frac{a_I}{a} \leq p_\varphi \leq \frac{m_\phi}{2} \right]. \end{aligned} \quad (3.15)$$

The reheaton number density can be expressed in the exact form,

$$n_\varphi(t) = \frac{1}{2\pi^2} \int f_\varphi(a, p_\varphi) p_\varphi^2 dp_\varphi = 6 \frac{M_P^2 H_I^2}{m_\phi} \left(\frac{a_I}{a(t)} \right)^3 \left[1 - e^{-\Gamma_\phi(t-t_I)} \right], \quad (3.16)$$

which can also be obtained from particle number conservation (that is, $(n_\phi + n_\varphi/2) a^3$ should be constant). The latter serves as a useful cross-check of Eq. (3.15).

Let us comment here that it could be possible for φ to reach kinetic equilibrium or even chemical equilibrium, dramatically changing the phase-space distribution previously computed. However, the former requires a sufficiently high elastic scattering rate of reheatoms $\varphi\varphi \rightarrow \varphi\varphi$, while the latter requires a particle-number-changing process such as $\varphi\varphi \rightarrow \varphi\varphi\varphi$. We have estimated the rates and find that they are in general below the Hubble expansion rate for the trilinear coupling strengths considered in this work.

3.3 Standard Model Thermal Bath

After inflatons decay to ultra-relativistic reheats, the Universe becomes radiation dominated. At a later epoch, they eventually release all their energy into SM particles through decays or annihilations, creating the SM thermal bath. As reheats are much lighter than inflatons, they are expected to decay at a much later time.⁴ Let us define $a = a_{\text{rh}}$ the scale factor at the equality between the energy density of reheats and the SM: $\rho_\varphi(a_{\text{rh}}) = \rho_{\text{SM}}(a_{\text{rh}})$, where

$$\rho_{\text{SM}}(T) = \frac{\pi^2}{30} g_\star(T) T^4, \quad (3.17)$$

with g_\star corresponding to the number of relativistic degrees of freedom contributing to ρ_{SM} . Therefore, the reheating temperature T_{rh} can be defined as $T_{\text{rh}} \equiv T(a_{\text{rh}})$. As the present analysis focuses on GWs with a non-thermal origin, the details of the SM thermal era are irrelevant, as long as the transition from φ to the SM content occurs when φ is *relativistic*.

The duration of the era dominated by reheats can be computed by the use of the scaling of the Hubble rate $H(a_\phi) a_\phi^2 = H(a_{\text{rh}}) a_{\text{rh}}^2$, which translates into

$$\frac{a_{\text{rh}}}{a_\phi} = \left[\frac{3}{\pi} \sqrt{\frac{10}{g_\star(T_{\text{rh}})}} \frac{M_P H_I}{T_{\text{rh}}^2} \left(\frac{a_I}{a_\phi} \right)^{\frac{3}{2}} \right]^{\frac{1}{2}}. \quad (3.18)$$

Furthermore, after the Universe fully transitions to the SM thermal plasma, the subsequent evolution follows the standard cosmological model in which the scale factor can be determined using the SM entropy conservation. In particular, between $T = T_{\text{rh}}$ and the present CMB temperature $T_0 \simeq 2.73 \text{ K} \simeq 0.23 \times 10^{-12} \text{ GeV}$ one has that

$$\frac{a_0}{a_{\text{rh}}} = \left[\frac{g_{\star s}(T_{\text{rh}})}{g_{\star s}(T_0)} \right]^{1/3} \frac{T_{\text{rh}}}{T_0}, \quad (3.19)$$

where a_0 is the scale factor at present, and $g_{\star s}(T)$ accounts for the effective degrees contributing to the SM entropy. Combining Eqs. (3.9), (3.18) and (3.19), one finds that

$$\begin{aligned} \frac{a_0}{a_I} &= \left(\frac{3}{\pi} \right)^{\frac{1}{2}} \left(\frac{10}{g_\star(T_{\text{rh}})} \right)^{\frac{1}{4}} \left(\frac{g_{\star s}(T_{\text{rh}})}{g_{\star s}(T_0)} \right)^{\frac{1}{3}} \left(\frac{1 + \gamma_\phi}{\gamma_\phi} \right)^{\frac{1}{6}} \frac{\sqrt{M_P H_I}}{T_0} \\ &\simeq 1.6 \times \left(\frac{1 + \gamma_\phi}{\gamma_\phi} \right)^{\frac{1}{6}} \frac{\sqrt{M_P H_I}}{T_0} \end{aligned} \quad (3.20)$$

which, as expected, is independent of T_{rh} (as long as T_{rh} is higher than the electroweak scale).

⁴Note that the decay or annihilation rate compared to the Hubble expansion rate is typically suppressed when the Universe is at a temperature much higher than all mass scales involved in the decay or annihilation process. For example, if φ has a small (compared to H_I and m_ϕ) mass m_φ above the electroweak scale, its decay rate is typically below $y^2 m_\varphi / (8\pi)$, with y being a dimensionless Yukawa coupling to SM fermions.

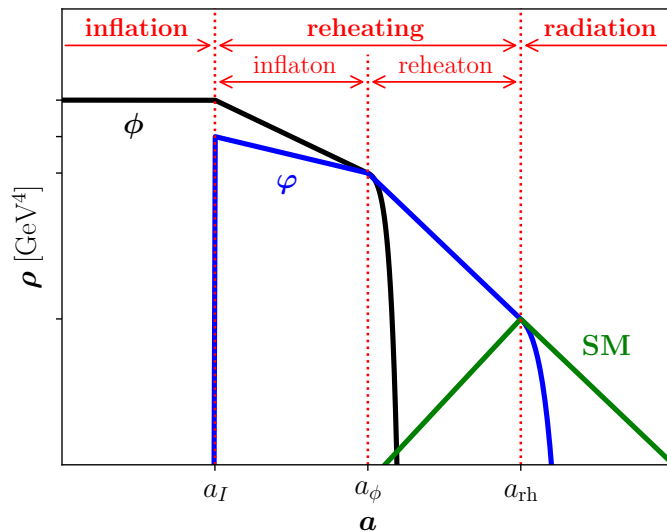


Figure 1. Artistic view of the evolution of the energy density of the different components of the Universe: inflaton ϕ in black, reheaton φ in blue, and SM in green. Cosmic inflation corresponds to $a < a_I$. Cosmic reheating occurs when $a_I < a < a_{\text{rh}}$, first dominated by the inflaton ($a_I < a < a_\phi$) and then by the reheaton ($a_{\text{rh}} < a < a_\phi$). Finally, the early Universe is dominated by SM radiation at $a_{\text{rh}} < a$.

Given that $a_{\text{rh}} \geq a_\phi$ within our model setup, we have the upper bound on T_{rh}

$$\begin{aligned}
 T_{\text{rh}} &\lesssim \sqrt{\frac{2}{\pi}} \left(\frac{10}{g_\star(T_{\text{rh}})} \right)^{1/4} \sqrt{M_P \Gamma_\phi} \\
 &\simeq 2.2 \times 10^{13} \left(\frac{10^{13} \text{ GeV}}{m_\phi} \right)^{1/2} \left(\frac{\mu}{10^{12} \text{ GeV}} \right) \text{ GeV}.
 \end{aligned} \tag{3.21}$$

The current upper bound on the reheating temperature is $T_{\text{rh}} \lesssim 5.5 \times 10^{15} \text{ GeV}$, which follows from the constraint on the inflationary Hubble scale, $H_I \lesssim 2.0 \times 10^{-5} M_P$, as inferred from the BICEP/Keck 2018 results [48]. We note that in the limit where $a_{\text{rh}} \rightarrow a_\phi$, that is, in the instantaneous decay scenario, we reproduce the usual result of T_{rh} . A lower bound on $T_{\text{rh}} \geq 4 \text{ MeV}$ also exists, coming from BBN [2–5, 49].

A sketch of the evolution of the energy density of the different components of the Universe is shown in Fig. 1: inflatons ϕ are shown in black, reheatoms φ in blue, and SM in green. Cosmic inflation corresponds to $a < a_I$. Cosmic reheating occurs when $a_I < a < a_{\text{rh}}$, first dominated by the inflaton ($a_I < a < a_\phi$) and then by the reheaton ($a_{\text{rh}} < a < a_\phi$). Finally, the Universe is dominated by SM radiation at $a_{\text{rh}} < a$, until the matter-radiation equality at $T \simeq 0.8 \text{ eV}$.

4 Gravitational Waves

In this work, we examine the graviton production from both inflatons and reheatoms. The corresponding Feynman diagrams are presented in Fig. 2. The first row (I) depicts graviton-pair production from inflaton annihilation. The second row (II) illustrates single-graviton

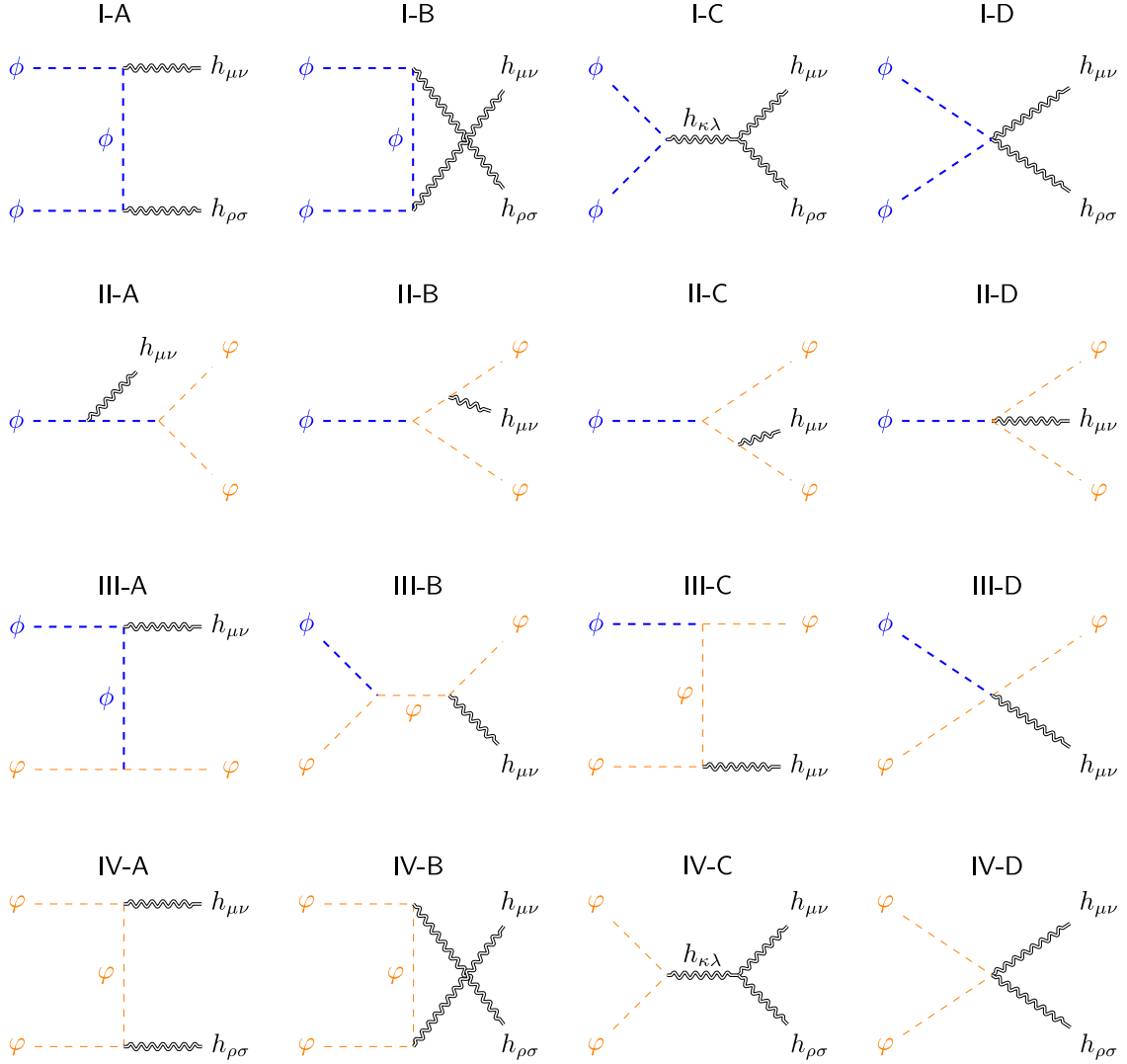


Figure 2. Feynman diagrams responsible for graviton ($h_{\mu\nu}$) production from inflatons (ϕ) and reheatons (φ), in the presence of the trilinear interaction in Eq. (2.3).

production via graviton Bremsstrahlung during inflaton decay into a pair of reheatons. The third row (III) represents inflaton-reheaton scattering, leading to the emission of a single graviton. Finally, the last row (IV) shows the production of graviton pairs from reheaton annihilations.⁵ This corresponds to all possible tree-level diagrams with at most four external particles.

We note that, beyond tree level, graviton production can also arise at loop level. For example, one can have the semi-annihilation of inflatons into an inflaton and a graviton, or the inflaton decay into a pair of gravitons. Processes with more external particles can also occur, such as 2-to-3 annihilations $\phi\phi \rightarrow \phi\phi h$, $\varphi\varphi \rightarrow \varphi\varphi h$, or $\phi\varphi \rightarrow \phi\varphi h$.

⁵We remind the reader that in the current setup with a minimal coupled Einstein-Hilbert action, there is no vertex between a single particle and two gravitons.

However, these production channels are further suppressed compared to direct inflaton annihilation [25].

The production of GWs from all the processes can be computed by solving the Boltzmann equation for the full phase-space distribution of gravitons

$$\frac{\partial f_h}{\partial t} - H p_h \frac{\partial f_h}{\partial p_h} = \Gamma_h, \quad (4.1)$$

where $f_h = f_h(a, p_h)$ is the phase-space distribution of the graviton $h_{\mu\nu}$ and Γ_h denotes the production rate of $h_{\mu\nu}$. The backreaction terms that account for the absorption of $h_{\mu\nu}$ via the inverse processes of those presented in Fig. 2 are not included, because they are negligible as long as $f_h \ll 1$. Consequently, the right-hand side of Eq. (4.1) is independent of f_h , allowing us to rewrite Eq. (4.1) into the integral form as

$$f_h(a, p_h) = \int_{a_I}^a \frac{da'}{a' H(a')} \Gamma_h \left(a', p_h \frac{a}{a'} \right). \quad (4.2)$$

It follows that the total energy density carried by GWs is

$$\rho_{\text{GW}}(a) = g_h \int \frac{4\pi p_h^3 dp_h}{(2\pi)^3} f_h(a, p_h), \quad (4.3)$$

where $g_h = 2$ denotes the two degrees of freedom for massless gravitons. The GW spectrum at present (that is, at $a = a_0$) is

$$\Omega_{\text{GW}}(f) \equiv \frac{1}{\rho_c} \frac{d\rho_{\text{GW}}(a_0)}{d \ln p_h} = 16\pi^2 \frac{f^4}{\rho_c} f_h(a_0, 2\pi f), \quad (4.4)$$

as a function of the frequency f of the GW, with $\rho_c \simeq 1.05 \times 10^{-5} h^2 \text{ GeV/cm}^3$ the critical energy density at present [50].

For a generic process, $X_1 + X_2 + \dots + X_n \rightarrow X_{n+1} + X_{n+2} + \dots + X_{n+m} + h$, the production rate (also known as the collision term) involves the $(n+m)$ -body phase space integral

$$\Gamma_h \equiv \frac{1}{2E_h} \int d\Pi_1 \dots d\Pi_{n+m} f_1 \dots f_n |\mathcal{M}|^2 (2\pi)^4 \delta^{(4)} \left(\sum_{i=1}^n p_i - \sum_{j=n+1}^{n+m} p_j \right), \quad (4.5)$$

where $d\Pi_i \equiv \frac{d^3 p_i}{(2\pi)^3 2E_i}$ is the Lorentz-invariant phase space with p_i and E_i the momentum and energy of the i^{th} particle in the process, f_i is the phase-space distribution of the i^{th} particle, and $(2\pi)^4 \delta^{(4)}(\dots)$ stands for the common delta function responsible for energy-momentum conservation.

Given the above formulae, it is possible to compute f_h and ρ_{GW} for the processes presented in Fig. 2. In the following, we discuss the production of GW in these processes and summarize the corresponding matrix elements and the production rates in Table 1.

Processes	Diagrams	S	$ \mathcal{M} ^2$	Γ_h
$\phi\phi \rightarrow hh$	I	$\frac{1}{4}$	$\frac{2m_\phi^4}{M_P^4}$	$\frac{\pi \mathcal{M} ^2 n_\phi^2}{16 E_h^2 m_\phi^2} \delta(E_h - m_\phi)$
$\phi \rightarrow \varphi\varphi h$	II	$\frac{1}{2}$	$\frac{2\mu^2}{M_P^2} \left(1 - \frac{m_\phi}{2E_h}\right)^2$	$\frac{ \mathcal{M} ^2 n_\phi}{64\pi m_\phi E_h}$
$\phi\varphi \rightarrow h\varphi$	III	1	$\frac{2\mu^2}{M_P^2} \left(1 - \frac{m_\phi}{2E_h}\right)^2$	Eq. (B.7)
$\varphi\varphi \rightarrow hh$	IV	$\frac{1}{4}$	$\frac{2t^2(s+t)^2}{M_P^4 s^2}$	$\frac{\pi n_\varphi^2}{320 E_h M_P^4}$

Table 1. Squared amplitudes $|\mathcal{M}|^2$, symmetry factors S and production rates Γ_h of gravitons for the processes presented in Fig. 2.

4.1 $\phi\phi \rightarrow hh$

At the end of inflation, the condensate of non-relativistic inflatons can directly produce gravitons via diagrams I-A to I-D in Fig. 2. The squared amplitude of this process can be obtained by taking the non-relativistic limit of the general calculation of GW production from scalar annihilation (see Eq. (A.18)) and is [24]

$$|\mathcal{M}_{\phi\phi \rightarrow hh}|^2 = \frac{2m_\phi^4}{M_P^4}; \quad (4.6)$$

the symmetry factor of the final and initial state is $S = 1/4$.

Since the squared amplitude is a constant, it can be moved outside the phase space integrals in Eq. (4.5). Labeling the particles in $\phi\phi \rightarrow hh$ from the left to the right by numbers 1 to 4, we compute Γ_h as follows:

$$\begin{aligned} \Gamma_h &= \frac{S}{2E_h} \int d\Pi_1 d\Pi_2 d\Pi_3 f_\phi(p_1) f_\phi(p_2) 2 |\mathcal{M}_{\phi\phi \rightarrow hh}|^2 (2\pi)^4 \delta^{(4)}(p_1 + p_2 - p_3 - p_4) \\ &= \frac{2S |\mathcal{M}_{\phi\phi \rightarrow hh}|^2}{2E_h} \int d\Pi_1 d\Pi_2 \frac{1}{2(E_1 + E_2 - E_h)} f_\phi(p_1) f_\phi(p_2) 2\pi \delta(E_1 + E_2 - 2E_h) \\ &= \frac{\pi S |\mathcal{M}_{\phi\phi \rightarrow hh}|^2 n_\phi^2}{8E_h^2 m_\phi^2} \delta(E_h - m_\phi) = \frac{\pi}{16} \frac{n_\phi^2}{M_P^4} \delta(E_h - m_\phi). \end{aligned} \quad (4.7)$$

Here $|\mathcal{M}_{\phi\phi \rightarrow hh}|^2$ in the first step is multiplied by a factor of two to account for the double graviton production; and in the last step we have used the cold condensate distribution in Eq. (3.4) for f_ϕ .

The corresponding phase-space distribution for the produced gravitons at the end of

the inflaton-dominated era is

$$\begin{aligned}
f_h(a_\phi, p_h) &= \int_{a_I}^{a_\phi} \frac{da'}{a' H(a')} \Gamma_h \left(a', p_h \frac{a_\phi}{a'} \right) \\
&= \frac{9\pi}{16} \frac{H_I^3}{m_\phi^2} \int_{a_I}^{a_\phi} \frac{da'}{a'} \delta \left(p_h \frac{a_\phi}{a'} - m_\phi \right) \left(\frac{a_I}{a'} \right)^{\frac{9}{2}} \exp \left[-\frac{4}{3} \frac{\Gamma_\phi}{H_I} \left(\frac{a'}{a_I} \right)^{\frac{3}{2}} \left[1 - \left(\frac{a_I}{a'} \right)^{\frac{3}{2}} \right] \right] \\
&= \frac{9\pi}{16} \left(\frac{H_I}{m_\phi} \right)^3 \left(\frac{a_I}{a_\phi} \frac{m_\phi}{p_h} \right)^{\frac{9}{2}} \exp \left[-\frac{4}{3} \frac{\Gamma_\phi}{H_I} \left[\left(\frac{a_\phi}{a_I} \frac{p_h}{m_\phi} \right)^{\frac{3}{2}} - 1 \right] \right] \\
&\quad \times \tilde{\Theta} \left(m_\phi \frac{a_I}{a_\phi} \leq p_h \leq m_\phi \right), \tag{4.8}
\end{aligned}$$

which allows to compute the spectrum of GWs. Furthermore, the total energy density in GWs at $a = a_\phi$

$$\begin{aligned}
\rho_{\text{GW}}(a_\phi) &= \int \frac{p_h^3 dp_h}{2\pi^2} f_h(a_\phi, p_h) \simeq \frac{9}{32\pi} H_I^3 \left(\frac{a_I}{a_\phi} \right)^3 \int_{m_\phi \frac{a_I}{a_\phi}}^{m_\phi} dp_h \left(\frac{a_I}{a_\phi} \frac{m_\phi}{p_h} \right)^{\frac{3}{2}} \\
&\simeq \frac{9}{16\pi} H_I^3 m_\phi \left(\frac{a_I}{a_\phi} \right)^4, \tag{4.9}
\end{aligned}$$

in agreement with Eq. (21) in Ref. [24], and Eq. (5.14) in Ref. [25] where a different method has been applied. The corresponding GW spectrum at present is

$$\Omega_{\text{GW}} h^2(f) \simeq 5.66 \times 10^{-20} \left(\frac{\mu}{10^{12} \text{ GeV}} \right)^{3/2} \left(\frac{m_\phi}{10^{13} \text{ GeV}} \right)^{3/4} \left(\frac{f}{10^7 \text{ Hz}} \right)^{-1/2}. \tag{4.10}$$

The graviton energy at production is the same as the inflaton mass, namely $E_h = m_\phi$. Once redshift is taken into account, the GW spectrum spans over the frequency band

$$f_{\min} \lesssim f \lesssim f_{\max}, \tag{4.11}$$

where

$$f_{\min} \simeq 6.4 \times 10^6 \left(\frac{m_\phi}{10^{13} \text{ GeV}} \right)^{5/6} \left(\frac{\mu}{10^{12} \text{ GeV}} \right)^{1/3} \left(\frac{2.0 \times 10^{-5} M_P}{H_I} \right)^{2/3} \text{ Hz} \tag{4.12}$$

$$f_{\max} \simeq 1.1 \times 10^{10} \left(\frac{m_\phi}{10^{13} \text{ GeV}} \right)^{3/2} \left(\frac{10^{12} \text{ GeV}}{\mu} \right) \text{ Hz}. \tag{4.13}$$

The GW spectrum with frequency above f_{\max} features a suppression factor $\sim e^{-(f/f_{\max})^2}$ due to the exponential suppression of the inflaton number density. We note that in a scenario where the inflaton decays into the reheaton directly reheats the Universe, the coupling can be expressed as a function of T_{rh} . In such a case, Eq. (4.10) reproduces the results given in Eq. (25) of Ref. [24] and Eq. (6.9) of Ref. [25]. Finally, we note that this is a purely gravitational channel and, therefore, its matrix element and corresponding collision term are independent of the trilinear coupling μ (cf. Eqs. (4.6) and (4.7)). However, its induced GW spectrum does have a dependence on μ through the redshift of the produced gravitons; cf. Eq. (4.10).

4.2 $\phi \rightarrow \varphi \varphi h$

When an inflaton ϕ decays into reheats φ , gravitons are unavoidably produced via Bremsstrahlung, as shown in II-A to D in Fig. 2. These diagrams lead to the following squared matrix element (see Eq. (A.31))

$$|\mathcal{M}_{\phi \rightarrow \varphi \varphi h}|^2 = \frac{2\mu^2}{M_P^2} \left(1 - \frac{m_\phi}{2E_h}\right)^2, \quad (4.14)$$

with the graviton energy E_h in the range $0 < E_h < \frac{m_\phi}{2}$; for higher energies the process is kinematically forbidden.

Since $|\mathcal{M}_{\phi \rightarrow \varphi \varphi h}|^2$ in this process depends only on E_h , it can be moved outside the phase-space integral, similar to the calculation of Γ_h in the previous subsection. Labeling the particles in $\phi \rightarrow \varphi \varphi h$ from the left to the right by numbers 1 to 4, Γ_h is then given by

$$\Gamma_h = \frac{|\mathcal{M}_{\phi \rightarrow \varphi \varphi h}|^2}{64\pi} \frac{n_\phi}{m_\phi p_h}, \quad (4.15)$$

see Section B.1 for further details.

The phase-space distribution for the produced gravitons at the end of the inflaton-dominated era is

$$f_h(a_\phi, p_h) \simeq \frac{1}{64\pi} \frac{\mu^2 H_I}{p_h^3} \left(\frac{a_I}{a_\phi}\right)^{\frac{3}{2}}, \quad (4.16)$$

while the total energy density stored in graviton at $a = a_\phi$ is

$$\rho_{\text{GW}}(a_\phi) = \int_0^{\frac{m_\phi}{2}} \frac{p_h^3 dp_h}{\pi^2} f_h(a_\phi, p_h) \simeq \frac{1}{128\pi^3} m_\phi \mu^2 H_I \left(\frac{a_I}{a_\phi}\right)^{\frac{3}{2}}, \quad (4.17)$$

which reproduces the result in Eq. (3.13) of Ref. [11] in the limit $a_\phi \rightarrow a_{\text{rh}}$, or in a scenario where inflatons directly decay into SM particles. The analytical expression for the GW can be written as

$$\Omega_{\text{GW}} h^2(f) \simeq 9.77 \times 10^{-21} \left(\frac{\mu}{10^{12} \text{ GeV}}\right) \left(\frac{m_\phi}{10^{13} \text{ GeV}}\right)^{\frac{1}{2}} \left(\frac{f}{10^7 \text{ Hz}}\right), \quad (4.18)$$

with $f \lesssim f_{\text{peak}} \simeq f_{\text{max}}/2$. It is interesting to note that, at its peak, the amplitude of the spectrum $\Omega_{\text{GW}}(f_{\text{peak}}) \propto m_\phi^2$, and only depends on m_ϕ . This implies that the lower m_ϕ , the smaller the GW amplitude would be. Similarly as in the previous case, higher frequency gravitons with $f > f_{\text{peak}}$ can also be generated, but the corresponding amplitude of the spectrum is exponentially suppressed. Finally, we note that in the case where reheating occurs through the coupling $\mu \phi \varphi^2$ (that is, φ is identified with the SM Higgs), Eq. (4.18) reproduces the result presented in Eq. (4.5) of Ref. [11].

4.3 $\phi \varphi \rightarrow \varphi h$

Gravitons can also be produced in 2-to-2 scatterings of inflatons with reheats, in a reheaton-catalyzed inflaton-to-graviton conversion. The corresponding diagrams are depicted in the third row of Fig. 2. The detailed computation of the squared amplitude

is presented in Appendix A.4, where we explicitly show that the squared amplitude of $\phi\varphi \rightarrow \varphi h$ is identical to that of $\phi \rightarrow \varphi\phi h$, as expected from crossing symmetries.

The calculation of Γ_h for $\phi\varphi \rightarrow \varphi h$ is similar to the calculation for $\phi \rightarrow \varphi\phi h$ in the previous subsection; however, in this case one has

$$\Gamma \sim \frac{\pi}{4} \frac{|\mathcal{M}|^2 n_\phi n_\varphi}{E_h^2 m_\phi^3} \tilde{\Theta} \left[\frac{1}{2} < \frac{E_h}{m_\phi} < 1 \right], \quad (4.19)$$

see Appendix B.2 for further details. The corresponding phase-space distribution for the produced gravitons at the end of the inflaton-dominated era can be approximated as

$$f_h(a_\phi, p_h) \simeq \frac{\pi}{4} \frac{M_P^2 \mu^2 H_I^2 \Gamma_\phi}{m_\phi^4 p_h^3} \left(\frac{a_I}{a_\phi} \right)^3 \quad (4.20)$$

for $\frac{m_\phi}{2} \frac{a_I}{a_\phi} < p_h < m_\phi$, which corresponds to a total energy density in the form of gravitons at $a = a_\phi$

$$\rho_{\text{GW}}(a_\phi) \simeq \frac{1}{4\pi} \frac{M_P^2 \mu^2 H_I^2 \Gamma_\phi}{m_\phi^3} \left(\frac{a_I}{a_\phi} \right)^3. \quad (4.21)$$

The GW spectrum is estimated as

$$\Omega_{\text{GW}} h^2(f) \simeq 5.86 \times 10^{-16} \left(\frac{\mu}{10^{12} \text{ GeV}} \right)^5 \left(\frac{10^{13} \text{ GeV}}{m_\phi} \right)^{\frac{11}{2}} \left(\frac{f}{10^7 \text{ Hz}} \right), \quad (4.22)$$

which also features a linear dependence on f in the low frequency regime, similar to the Bremsstrahlung spectrum. At peak, the spectrum $\Omega_{\text{GW}}(f_{\text{peak}}) \propto (\mu/m_\phi)^4$, being constant if $\mu \propto m_\phi$. Similarly to the previous case, the frequency is in the range $2 f_{\text{min}} \lesssim f \lesssim f_{\text{max}}$.

Before closing this section, we emphasize that the GW spectrum previously computed corresponds to a *non-thermal* reheaton. For a thermalized reheaton, the spectrum starts at lower frequencies and has a much suppressed amplitude, due to the change in the phase-space distribution [25].

4.4 $\varphi\varphi \rightarrow hh$

Pairs of gravitons can also be produced by annihilations of ultra-relativistic reheatons, see the fourth line of Fig. 2. In the ultra-relativistic limit, the squared amplitude in Eq. (A.17) reduces to [33]

$$|\mathcal{M}_{\varphi\varphi \rightarrow hh}|^2 = \frac{2t^2 (s+t)^2}{M_P^4 s^2}. \quad (4.23)$$

An exact analytical expression for the production rate Γ_h for this channel is challenging to obtain due to the integration over the phase space. However, we estimate it to be

$$\Gamma_h \simeq \frac{\pi}{320} \frac{n_\varphi^2}{M_P^4 E_h}, \quad (4.24)$$

where $\frac{m_\phi}{2} \frac{a_I}{a} < E_h < \frac{m_\phi}{2} \times \min(1, a_\phi/a)$. The exact collision term Γ_h can always be obtained numerically. The phase-space distribution of gravitons at $a = a_\phi$ is

$$f_h(a_\phi, p_h) \simeq \frac{9\pi}{140} \frac{H_I \Gamma_\phi^2 a_I}{m_\phi^2 p_h a_\phi}, \quad (4.25)$$

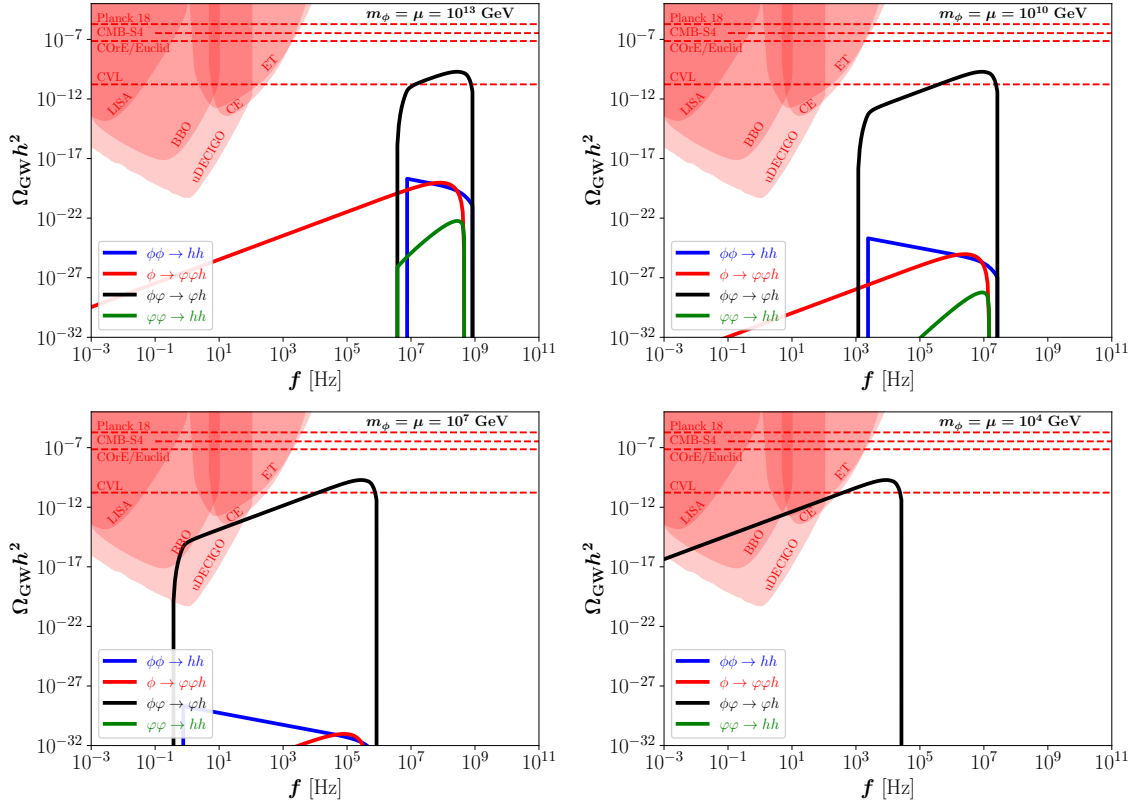


Figure 3. Comparison of the different sources of GWs, for $m_\phi = 10^{13}$ GeV, 10^{10} GeV, 10^7 GeV and 10^4 GeV, assuming $H_I = 2.0 \times 10^{-5} M_P$ and $m_\phi = \mu$.

for $\frac{m_\phi}{2} \frac{a_I}{a} < p_h < \frac{m_\phi}{2} \times \min(1, a_\phi/a)$. The total energy density for GW can be estimated as

$$\rho_{\text{GW}}(a_\phi) \simeq \frac{3}{1120\pi} H_I m_\phi \Gamma_\phi^2 \frac{a_I}{a_\phi}. \quad (4.26)$$

Finally, the differential GW spectrum can be approximated as

$$\Omega_{\text{GW}} h^2(f) \simeq 1.32 \times 10^{-29} \left(\frac{H_I}{2.0 \times 10^{-5} M_P} \right)^{\frac{1}{3}} \left(\frac{\mu}{10^{12} \text{ GeV}} \right)^{\frac{13}{3}} \left(\frac{10^{13} \text{ GeV}}{m_\phi} \right)^{\frac{25}{6}} \left(\frac{f}{10^7 \text{ Hz}} \right)^3 \quad (4.27)$$

for $f_{\text{min}}/2 \lesssim f < f_{\text{max}}/2$. This contribution is lower than the spectrum produced from pure inflaton-inflaton annihilation; cf. Eq. (4.10). The difference arises because the graviton production rate in the former case is smaller than in the latter. In particular, the spectrum exhibits a f^3 dependence, similar to the GW spectrum generated by relativistic SM degrees of freedom in a thermal plasma [26–29].

4.5 Comparison

A comparison of the different GW spectra is presented in Fig. 3, for $m_\phi = 10^{13}$ GeV, 10^{10} GeV, 10^7 GeV and 10^4 GeV, assuming $H_I = 2.0 \times 10^{-5} M_P$, and $\mu = m_\phi$, close to the unitarity bound. The four GW spectra of the tree-level processes with at most four external

particles described previously are presented separately: $\phi\phi \rightarrow hh$ (blue), $\phi \rightarrow \varphi\varphi h$ (red), $\phi\varphi \rightarrow \varphi h$ (black), and $\varphi\varphi \rightarrow hh$ (green).

In Fig. 3, we also present the sensitivity curves of several proposed GW detectors, including the Laser Interferometer Space Antenna (LISA) [51], the Einstein Telescope (ET) [52–55], the Cosmic Explorer (CE) [56], the Big Bang Observer (BBO) [57–59], and the ultimate DECIGO (uDECIGO) [60, 61]. The energy stored in GWs behaves similarly to dark radiation, contributing to the effective number of neutrino species, N_{eff} .⁶ To illustrate these constraints, we include horizontal dashed red lines in Fig. 3. The Planck 2018 mission provides a 95% CL measurement of $N_{\text{eff}} = 2.99 \pm 0.34$ [62]. Future experiments, such as CORe [63] and Euclid [64], are expected to improve these constraints to $\Delta N_{\text{eff}} \lesssim 0.013$ at the 2σ level. The next-generation CMB experiment, CMB-S4, is projected to achieve a sensitivity of $\Delta N_{\text{eff}} \lesssim 0.06$ [65]. Additionally, we include a limit of $\Delta N_{\text{eff}} \lesssim 3 \times 10^{-6}$, reported in Ref. [66], based on a hypothetical cosmic-variance-limited (CVL) CMB polarization experiment.

Concerning Fig. 3, we start with the upper left panel, where $m_\phi = \mu = 10^{13}$ GeV. Some comments are in order: *i*) We find that GWs from the channel $\phi\varphi \rightarrow \varphi h$ exhibit the highest amplitude and have a linear dependency on f , which can reach $\Omega_{\text{GW}} \sim \mathcal{O}(10^{-11})$, within the sensitivity of a CVL experiment. *ii*) The spectra from $\phi\varphi \rightarrow \varphi h$ and $\varphi\varphi \rightarrow hh$ are similar; however, double graviton production has a smaller amplitude due to the additional $1/M_{\text{P}}^2$ suppression. *iii*) The non-thermal nature of the reheaton (that is, a very large phase-space distribution over a narrow energy band) renders the spectrum from $\phi\varphi \rightarrow \varphi h$ to higher amplitudes and to a smaller frequency range with respect to the Bremsstrahlung $\phi \rightarrow \varphi\varphi h$, even if they share the same matrix element. *iv*) The GW spectrum from $\phi\phi \rightarrow hh$ annihilation is larger than that from $\varphi\varphi \rightarrow hh$ scatterings. The former follows an $f^{-1/2}$ scaling, mainly due to the non-relativistic nature of the inflaton, whereas the latter exhibits an f^3 behavior, similar to GWs generated from relativistic degrees of freedom in the SM thermal bath.

A decrease in the inflaton mass reduces the energy of the gravitons produced, and therefore the GW spectra move to lower frequencies. In addition, a decrease in μ translates into a longer reheating era dominated by reheatons (cf. Eq. (3.9)) and, in turn, a broad range of frequencies for $\phi\phi \rightarrow hh$, $\phi\varphi \rightarrow \varphi h$ and $\varphi\varphi \rightarrow hh$. For $\mu = m_\phi$, all spectra shift to lower frequencies. However, amplitudes are also reduced, as shown in the upper right and lower panels of Fig. 3. Interestingly, in the particular case where $\mu \propto m_\phi$, the maximal amplitude of the spectrum from $\phi\varphi \rightarrow \varphi h$ remains unchanged, since it scales as $(\mu/m_\phi)^4$; cf. Eq. (4.22). It is remarkable that for sufficiently light inflaton masses ($m_\phi \lesssim 10^7$ GeV), the spectrum from $\phi\varphi \rightarrow \varphi h$ falls within the sensitivity of future GW experiments, such as ET, CE, uDECIGO and BBO.

In Fig. 4, we consider a scenario with a smaller trilinear coupling μ with respect to the inflaton mass: $\mu = m_\phi/10$. As expected, the amplitudes of all spectra reduce, and the frequencies span over a larger range. Similarly to the previous case, the GWs produced

⁶For the constraint from N_{eff} , we use $\Omega_{\text{GW}} h^2 \lesssim 5.6 \times 10^{-6} \Delta N_{\text{eff}}$, which applies to the integrated energy density over logarithmic frequency [1].

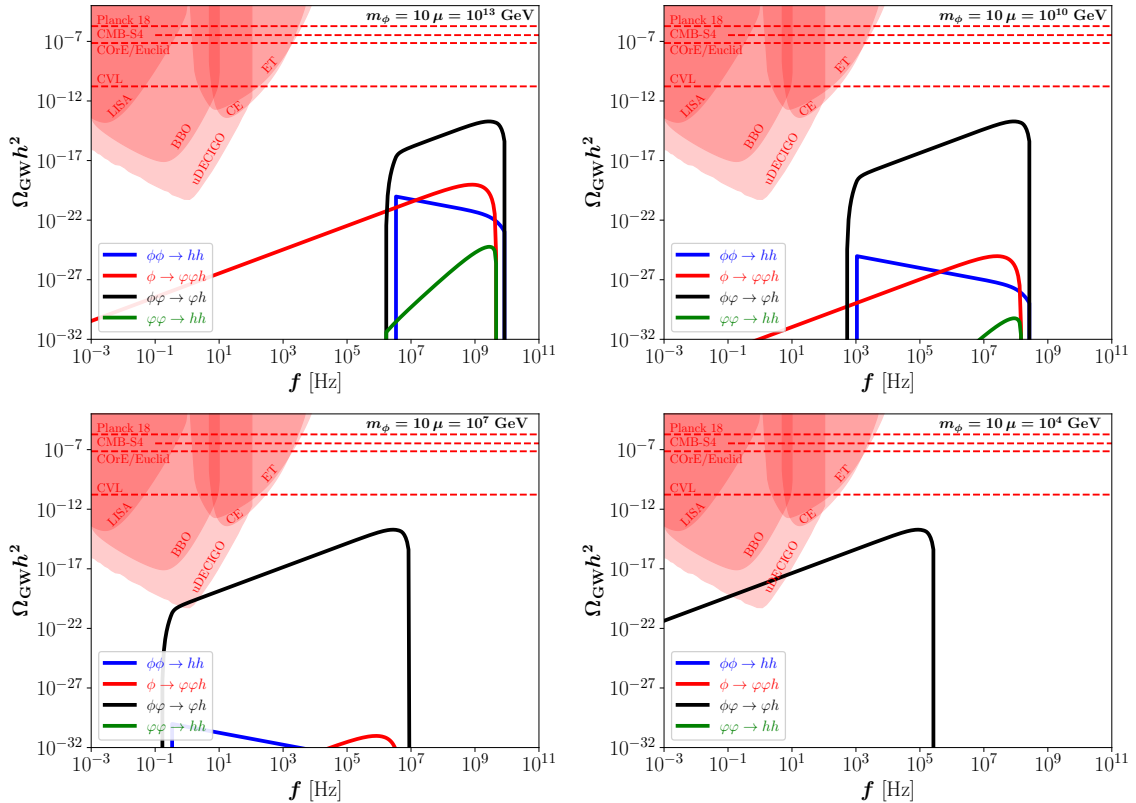


Figure 4. Comparison of the different sources of GWs. Equivalent of Fig. 3 but for $\mu = m_\phi/10$.

from $\phi\phi \rightarrow \phi h$ have the largest amplitude. In this scenario, the GW spectrum could fall within the sensitivity of uDECIGO for a light inflaton with mass $m_\phi \lesssim 10^7$ GeV.

Before closing, we comment on the effect of H_I . For the GW spectrum from $\phi\phi \rightarrow \phi h$, the peak is determined by m_ϕ and μ (cf. Eq. (4.22)) and is independent of the inflationary scale H_I . Instead, H_I governs the frequency band range, as shown in Eq. (4.11). A smaller H_I shifts the lower limit f_{\min} upward, narrowing the frequency range.

5 Conclusions

In this work, a novel gravitational wave (GW) production mechanism is explored for the first time, where gravitons are generated during the *non-thermal* phase of the cosmic reheating era. We consider a scenario in which reheating occurs via inflaton decays into a weakly coupled intermediate state (i.e. the reheatons), which subsequently transfer their energy to Standard Model (SM) degrees of freedom, leading to the formation of a thermal SM bath. Before thermalization is complete, a large population of highly energetic reheatons emerges, with energies comparable to the inflaton mass. During this phase, GWs are generated through multiple production channels: *i*) pure inflaton-inflaton annihilation, *ii*) graviton Bremsstrahlung from inflaton decays to reheatons, *iii*) scatterings between an inflaton and a reheaton, and *iv*) scatterings among reheatons.

We systematically analyze each channel and determine the resulting GW spectrum by solving the Boltzmann equation at the graviton phase-space distribution level. This approach, which has not been previously applied in this context, provides a robust framework that reproduces known results for inflaton-inflaton annihilation and graviton Bremsstrahlung. More notably, we find that the third channel (that is, the reheaton-catalyzed inflaton-to-graviton conversion) leads to a significantly larger amplitude of the GW signal because of the abundance of hard, *non-thermal* reheatons in the initial state. Our main results, summarized in Figs. 3 and 4, compare the contributions of different GW production mechanisms. Interestingly, in scenarios with a low inflaton mass ($m_\phi \lesssim 10^7$ GeV), the GW spectrum could lie within the sensitivity range of future experiments such as the Einstein Telescope (ET), Cosmic Explorer (CE), Big Bang Observer (BBO), and ultimate DECIGO (uDECIGO).

In summary, we have identified a novel perturbative source of GWs arising during the pre-thermalization phase of cosmic reheating. The resulting GW signal could be probed by future experiments.

Acknowledgments

NB acknowledges the Institute of High Energy Physics and the Chinese Academy of Sciences for their hospitality. NB received funding from the grants PID2023-151418NB-I00 funded by MCIU/AEI/10.13039/501100011033/FEDER and PID2022-139841NB-I00 of MCIU/AEI/10.13039/501100011033 and FEDER, UE. The work of XJX is supported in part by the National Natural Science Foundation of China (NSFC) under grant No. 12141501 and also by the CAS Project for Young Scientists in Basic Research (YSBR-099). YX has received support from the Cluster of Excellence “Precision Physics, Fundamental Interactions, and Structure of Matter” (PRISMA⁺ EXC 2118/1) funded by the Deutsche Forschungsgemeinschaft (DFG, German Research Foundation) within the German Excellence Strategy (Project No. 390831469).

A Calculation of $|\mathcal{M}|^2$

In this appendix, we present squared amplitudes for several processes discussed in the main text. For reproducibility, we provide the WOLFRAM MATHEMATICA notebooks that include the derivations of the Feynman rules for the vertices and the calculations of the squared amplitudes, which are available on [GitHub](https://github.com/Fenyutanchan/amplitude-for-inflaton-reheaton-graviton).⁷

A.1 Gravitational Polarization Summation

We work in the transverse and traceless gauge with $\omega_\mu \epsilon^{\mu\nu} = 0$ and $\eta_{\mu\nu} \epsilon^{\mu\nu} = \epsilon^\mu{}_\mu = 0$, where ω_μ denotes the four-momentum of graviton and $\epsilon^{\mu\nu}$ denotes its polarization tensor. The polarization sum reads

$$\sum_{\text{pol}} \epsilon^{*\mu\nu} \epsilon^{\alpha\beta} = \frac{1}{2} \left(\hat{\eta}^{\mu\alpha} \hat{\eta}^{\nu\beta} + \hat{\eta}^{\mu\beta} \hat{\eta}^{\nu\alpha} - \hat{\eta}^{\mu\nu} \hat{\eta}^{\alpha\beta} \right), \quad (\text{A.1})$$

⁷<https://github.com/Fenyutanchan/amplitude-for-inflaton-reheaton-graviton>

with

$$\hat{\eta}_{\mu\nu} \equiv \eta_{\mu\nu} - \frac{\omega_\mu \bar{\omega}_\nu + \bar{\omega}_\mu \omega_\nu}{\omega \cdot \bar{\omega}}, \quad (\text{A.2})$$

where $\omega = (E_\omega, \vec{\omega})$ and $\bar{\omega} = (E_\omega, -\vec{\omega})$.

A.2 Graviton Production from Scalar Annihilation

A pair of gravitons can be generated from the annihilation of a pair of scalars such as inflatons or reheatons, as already shown in Fig. 2. We label the momenta of the two initial scalars by p_1 and p_2 , and the momenta of the two final gravitons by p_3 and p_4 , respectively. Therefore, the Mandelstam variables are given by $s = (p_1 + p_2)^2$, $t = (p_1 - p_3)^2$, and $u = (p_1 - p_4)^2$ with $s + t + u = 2m^2$, where m denotes the scalar mass, it being m_ϕ or m_φ . The matrix elements of diagrams I-A to I-D (or IV-A to IV-D) in Fig. 2 read

$$i\mathcal{M}_t = \frac{-i}{M_P} (2 p_{1\mu} p_{1\nu}) \frac{i}{t - m^2} \frac{-i}{M_P} (2 p_{2\lambda} p_{2\kappa}) \epsilon^{*\mu\nu} \epsilon^{*\lambda\kappa}, \quad (\text{A.3})$$

$$i\mathcal{M}_u = \frac{-i}{M_P} (2 p_{1\lambda} p_{1\kappa}) \frac{i}{u - m^2} \frac{-i}{M_P} (2 p_{2\mu} p_{2\nu}) \epsilon^{*\mu\nu} \epsilon^{*\lambda\kappa}, \quad (\text{A.4})$$

$$i\mathcal{M}_s = \frac{2i}{M_P} [2 p_{1\rho} p_{2\sigma} - \eta_{\rho\sigma} (m^2 + p_1 \cdot p_2)] \frac{i}{2s} [\eta_{\rho\alpha} \eta_{\sigma\beta} + \eta_{\rho\beta} \eta_{\sigma\alpha} - \eta_{\alpha\beta} \eta_{\rho\sigma}] V_{\alpha\beta\mu\nu\lambda\kappa} \epsilon^{*\mu\nu} \epsilon^{*\lambda\kappa}, \quad (\text{A.5})$$

$$i\mathcal{M}_4 = \frac{i}{M_P^2} [\eta_{\mu\nu} \eta_{\lambda\kappa} - \eta_{\mu\lambda} \eta_{\nu\kappa} - \eta_{\mu\kappa} \eta_{\nu\lambda}] (-p_1 \cdot p_2 - m^2) \\ + [2(\eta_{\nu\lambda} p_{2\mu} p_{2\kappa} + \eta_{\mu\kappa} p_{2\lambda} p_{2\nu} + \eta_{\mu\lambda} p_{2\nu} p_{2\kappa} + \eta_{\nu\kappa} p_{2\lambda} p_{2\mu})] \epsilon^{*\mu\nu} \epsilon^{*\lambda\kappa}, \quad (\text{A.6})$$

where $V_{\alpha\beta\mu\nu\lambda\kappa}$ denotes the triple-graviton vertex. The corresponding Feynman rules can be found in Ref. [39]. Note that any term with $p_{3\alpha}$, $p_{3\beta}$, $p_{4\gamma}$, $p_{4\delta}$, $\eta_{\alpha\beta}$, or $\eta_{\gamma\delta}$ would vanish in the matrix element once combined with the graviton polarization tensors due to the

transverse condition and traceless condition. We find

$$|\mathcal{M}_t|^2 = \frac{4 \left[m^4 - 2m^2t + t(s+t) \right]^4}{M_P^4 s^4 (m^2 - t)^2}, \quad (\text{A.7})$$

$$|\mathcal{M}_u|^2 = \frac{4 \left[m^4 - 2m^2u + u(s+u) \right]^4}{M_P^4 s^4 (m^2 - u)^2}, \quad (\text{A.8})$$

$$|\mathcal{M}_s|^2 = \frac{2 (s^2 + 3st + 3t^2)^2}{M_P^4 s^2}, \quad (\text{A.9})$$

$$|\mathcal{M}_4|^2 = \frac{2 \left[4m^4 - 8m^2t + (s+2t)^2 \right]^2}{M_P^4 s^2}, \quad (\text{A.10})$$

$$\mathcal{M}_s \mathcal{M}_t^* = \frac{-2 \left[m^4 - 2m^2t + t(s+t) \right]^2 \left[3m^4 - m^2(s+6t) + s^2 + 3st + 3t^2 \right]}{M_P^4 s^3 (m^2 - t)}, \quad (\text{A.11})$$

$$\mathcal{M}_s \mathcal{M}_u^* = \frac{-2 \left[m^4 - 2m^2t + t(s+t) \right]^2 \left[3m^4 - m^2(s+6t) + s^2 + 3st + 3t^2 \right]}{M_P^4 s^3 (s+t-m^2)}, \quad (\text{A.12})$$

$$\mathcal{M}_s \mathcal{M}_4^* = \frac{-2 \left[4m^4 - 8m^2t + (s+2t)^2 \right] \left[3m^4 - m^2(s+6t) + s^2 + 3st + 3t^2 \right]}{M_P^4 s^2}, \quad (\text{A.13})$$

$$\mathcal{M}_t \mathcal{M}_u^* = \frac{4 \left[m^4 - 2m^2t + t(s+t) \right]^4}{M_P^4 s^4 (m^2 - t)(s+t-m^2)}, \quad (\text{A.14})$$

$$\mathcal{M}_t \mathcal{M}_4^* = \frac{2 \left[m^4 - 2m^2t + t(s+t) \right]^2 \left[4m^4 - 8m^2t + (s+2t)^2 \right]}{M_P^4 s^3 (m^2 - t)}, \quad (\text{A.15})$$

$$\mathcal{M}_u \mathcal{M}_4^* = \frac{2 \left[m^4 - 2m^2t + t(s+t) \right]^2 \left[4m^4 - 8m^2t + (s+2t)^2 \right]}{M_P^4 s^3 (s+t-m^2)}. \quad (\text{A.16})$$

The total squared matrix elements are

$$\begin{aligned} |\mathcal{M}|^2 &= |\mathcal{M}_s + \mathcal{M}_t + \mathcal{M}_u + \mathcal{M}_4|^2 \\ &= |\mathcal{M}_s|^2 + |\mathcal{M}_t|^2 + |\mathcal{M}_u|^2 + |\mathcal{M}_4|^2 \\ &\quad + 2(\mathcal{M}_s \mathcal{M}_t^* + \mathcal{M}_s \mathcal{M}_u^* + \mathcal{M}_s \mathcal{M}_4^* + \mathcal{M}_t \mathcal{M}_u^* + \mathcal{M}_t \mathcal{M}_4^* + \mathcal{M}_u \mathcal{M}_4^*) \\ &= \frac{2}{s^2 (t-m^2)^2 (s+t-m^2)^2 M_P^4} \\ &\quad \times \left[m^{16} - 8m^{14}t + 4m^{12}t(s+7t) - 8m^{10}t^2(3s+7t) \right. \\ &\quad \left. + m^8 (s^4 + 6s^2t^2 + 60st^3 + 70t^4) - 8m^6t^3(s+t)(3s+7t) \right. \\ &\quad \left. + 4m^4t^3(s+t)^2(s+7t) - 8m^2t^4(s+t)^3 + t^4(s+t)^4 \right]. \end{aligned} \quad (\text{A.17})$$

We notice that Eq. (A.17) is more general compared to the existing ones in the literature. For non-relativistic inflatons annihilating into gravitons, we have

$$|\mathcal{M}_{\phi\phi \rightarrow hh}|^2 = \frac{2m_\phi^4}{M_P^4}, \quad (\text{A.18})$$

thus reproducing the result presented in Ref. [24]. For relativistic reheatons annihilating into gravitons, Eq. (A.17) reduces to

$$|\mathcal{M}_{\varphi\varphi\rightarrow hh}|^2 = \frac{2t^2(s+t)^2}{M_P^4 s^2}, \quad (\text{A.19})$$

which agrees with Eq. (25) in Ref. [33].

A.3 Graviton Production from Bremsstrahlung

For momenta labeled as $\phi(l) \rightarrow \varphi(p) \varphi(q) h_{\mu\nu}(\omega)$, the matrix elements are [11]

$$i\mathcal{M}_1 = -\frac{i\mu}{M_P} \frac{l_\mu l_\nu \epsilon^{*\mu\nu}}{l \cdot \omega}, \quad (\text{A.20})$$

$$i\mathcal{M}_2 = +\frac{i\mu}{M_P} \frac{p_\mu p_\nu \epsilon^{*\mu\nu}}{p \cdot \omega}, \quad (\text{A.21})$$

$$i\mathcal{M}_3 = +\frac{i\mu}{M_P} \frac{q_\mu q_\nu \epsilon^{*\mu\nu}}{q \cdot \omega}, \quad (\text{A.22})$$

$$i\mathcal{M}_4 \propto \eta_{\mu\nu} \epsilon^{\mu\nu} = 0, \quad (\text{A.23})$$

for the initial-state graviton emitted from the inflaton (\mathcal{M}_1), the final-state reheatons (\mathcal{M}_2 and \mathcal{M}_3) and the vertex (\mathcal{M}_4), respectively. The last matrix element \mathcal{M}_4 vanishes due to the traceless condition of the graviton polarization tensor. Moreover, the matrix element \mathcal{M}_1 vanishes since the inflaton is at rest, that is, $l = (m_\phi, \vec{0})$. This, in other words, implies that the source of GW in this case is $T_\phi^{ij} = 0$, as commented just below Eq. (2.8). Note that T^{ij} in momentum space corresponds to the three-momentum. Another way to see this is to directly compute the squared matrix element $|\mathcal{M}_1|^2$, and we find

$$|\mathcal{M}_1|^2 = \frac{\mu^2 [l^2(\omega \cdot \bar{\omega}) - 2(l \cdot \omega)(l \cdot \bar{\omega})]^2}{2M_P^2 (l \cdot \omega)^2 (\omega \cdot \bar{\omega})^2}, \quad (\text{A.24})$$

which is $\frac{\mu^2 [2m_\phi^2 E_\omega^2 - 2m_\phi^2 E_\omega^2]^2}{8M_P^2 E_\omega^2 m_\phi^2 E_\omega^4} = 0$ in the non-relativistic limit of the inflaton. Note that \mathcal{M}_2 and \mathcal{M}_3 do not vanish because the produced reheatons φ are not at rest. An equivalent argument would be the source of GW $T_\phi^{ij} \neq 0$.

Using the conservation of four momentum $l = p + q + \omega$ and the transverse condition of graviton, we notice that the third diagram can be smartly rewritten as

$$i\mathcal{M}_3 = \frac{+i\mu}{M_P} \frac{p_\mu p_\nu \epsilon^{*\mu\nu}}{(l-p) \cdot \omega}, \quad (\text{A.25})$$

which greatly simplifies the calculation. We find

$$|\mathcal{M}_2|^2 = \frac{\mu^2 [p^2(\omega \cdot \bar{\omega}) - 2(p \cdot \omega)(p \cdot \bar{\omega})]^2}{2M_P^2 (p \cdot \omega)^2 (\omega \cdot \bar{\omega})^2}, \quad (\text{A.26})$$

$$|\mathcal{M}_3|^2 = \frac{\mu^2 [p^2(\omega \cdot \bar{\omega}) - 2(p \cdot \omega)(p \cdot \bar{\omega})]^2}{2M_P^2 (l \cdot \omega - p \cdot \omega)^2 (\omega \cdot \bar{\omega})^2}, \quad (\text{A.27})$$

$$\mathcal{M}_2 \mathcal{M}_3^* = \frac{\mu^2 [p^2(\omega \cdot \bar{\omega}) - 2(p \cdot \omega)(p \cdot \bar{\omega})]^2}{2M_P^2 (p \cdot \omega)(l \cdot \omega - p \cdot \omega)(\omega \cdot \bar{\omega})^2}, \quad (\text{A.28})$$

and the total squared matrix element is

$$\begin{aligned}
|\mathcal{M}_{\phi \rightarrow \varphi \varphi h}|^2 &= |\mathcal{M}_2|^2 + |\mathcal{M}_3|^2 + 2\mathcal{M}_2\mathcal{M}_3^* = \frac{\mu^2}{2M_P^2} \frac{(l \cdot \omega)^2 [p^2(\omega \cdot \bar{\omega}) - 2(p \cdot \omega)(p \cdot \bar{\omega})]^2}{(l \cdot \omega - p \cdot \omega)^2 (p \cdot \omega)^2 (\omega \cdot \bar{\omega})^2} \\
&\simeq \frac{2\mu^2}{M_P^2} \frac{(l \cdot \omega)^2 (p \cdot \bar{\omega})^2}{(l \cdot \omega - p \cdot \omega)^2 (\omega \cdot \bar{\omega})^2} = \frac{2\mu^2}{M_P^2} \frac{(l \cdot \omega)^2 (p \cdot \bar{\omega})^2}{(q \cdot \omega)^2 (\omega \cdot \bar{\omega})^2}, \tag{A.29}
\end{aligned}$$

where in the last second step we have taken $m_\varphi \rightarrow 0$. We also note that our result is invariant under $p \leftrightarrow q$ as expected.

Without loss of generality, we take $\omega^\mu = (E_h, E_h, 0, 0)$, $\bar{\omega}^\mu = (E_h, -E_h, 0, 0)$, $l^\mu = (m_\phi, 0, 0, 0)$, and $p^\mu = (E_p, p_x, p_y, p_z)$. Then using the on-shell conditions of p^μ and q^μ ($p \cdot p = q \cdot q = 0$) as well as $l \cdot p = m_\phi E_p$ and $l \cdot \omega = m_\phi E_h$, it is straightforward to express E_h , E_p , p_x , and $p_y^2 + p_z^2$ in terms of $l \cdot p$, $l \cdot \omega$, $p \cdot p$, and $q \cdot q$. This allows us to further obtain

$$\frac{p \cdot \bar{\omega}}{q \cdot \omega} = 1 - 2 \frac{l \cdot \omega}{m_\phi^2} = 1 - 2 \frac{E_h}{m_\phi}, \tag{A.30}$$

and simplify Eq. (A.29) to

$$|\mathcal{M}_{\phi \rightarrow \varphi \varphi h}|^2 = \frac{2\mu^2}{M_P^2} \left(1 - \frac{m_\phi}{2E_h}\right)^2. \tag{A.31}$$

A.4 Graviton Production from Inflaton and Reheaton Scattering

For momenta labeled as $\phi(l) \varphi(q) \rightarrow \varphi(p) h_{\mu\nu}(\omega)$, and the matrix elements are [25]

$$i\mathcal{M}_u = -\frac{i\mu}{M_P} \frac{l_\mu l_\nu \epsilon^{*\mu\nu}}{l \cdot \omega}, \tag{A.32}$$

$$i\mathcal{M}_s = +\frac{i\mu}{M_P} \frac{p_\mu p_\nu \epsilon^{*\mu\nu}}{p \cdot \omega}, \tag{A.33}$$

$$i\mathcal{M}_t = -\frac{i\mu}{M_P} \frac{q_\mu q_\nu \epsilon^{*\mu\nu}}{q \cdot \omega}, \tag{A.34}$$

$$i\mathcal{M}_4 \propto \eta_{\mu\nu} \epsilon^{\mu\nu} = 0, \tag{A.35}$$

where the last matrix element \mathcal{M}_4 vanishes due to the traceless condition for graviton polarization tensor. We note if changing the reheaton φ from the initial state to the final state, we reproduce the case $1 \rightarrow 3$ in the previous subsection. Consequently, the matrix elements for these $2 \rightarrow 2$ scatterings are similar to those presented in the previous case of $1 \rightarrow 3$ Bremsstrahlung, except that there is an extra minus sign in \mathcal{M}_t compared to \mathcal{M}_3 .

We define Mandelstam variables as $s = (l + q)^2$, $t = (l - p)^2$, and $u = (l - \omega)^2$ with $s + t + u = 2m_\varphi^2 + m_\phi^2$. The general total squared matrix element is shown to be:

$$|\mathcal{M}_{\phi \rightarrow \varphi \varphi h}|^2 = \frac{2\mu^2 \left[2m_\varphi^6 - m_\varphi^4 (m_\phi^2 + s + t) + m_\varphi^2 (m_\phi^2 (s + t) - 2st) + st(s + t - m_\phi^2) \right]^2}{M_P^2 (s - m_\varphi^2)^2 (t - m_\varphi^2)^2 (s + t - 2m_\varphi^2)^2}. \tag{A.36}$$

In the limit of ultra-relativistic reheats ($m_\phi \rightarrow 0$), it reduces to

$$|\mathcal{M}_{\phi\phi\rightarrow\varphi h}|^2 = \frac{2\mu^2(s+t-m_\phi^2)^2}{M_P^2(s+t)^2}. \quad (\text{A.37})$$

Additionally, if one further demands non-relativistic inflatons, $l = (m_\phi, 0, 0, 0)$, we have $u = (l - \omega)^2 = m_\phi^2 - 2l \cdot \omega = m_\phi^2 - 2m_\phi E_h$. Then using $s + t = m_\phi^2 - u$, we can simply Eq. (A.36) as

$$|\mathcal{M}_{\phi\phi\rightarrow\varphi h}|^2 = \frac{\mu^2}{2M_P^2} \left(2 - \frac{m_\phi}{E_h}\right)^2, \quad (\text{A.38})$$

which matches Eq. (A.31) and agrees with Ref. [25].

Finally, we note here that \mathcal{M}_u vanishes for non-relativistic ϕ . This can also be easily seen by noticing that

$$|\mathcal{M}_u|^2 = \frac{2\mu^2 [l^2(\omega \cdot \bar{\omega}) - 2(l \cdot \omega)(l \cdot \bar{\omega})]^2}{M_P^2(u - m_\phi^2)^2(\omega \cdot \bar{\omega})^2} = \frac{2\mu^2 [2m_\phi^2 E_h^2 - 2m_\phi^2 E_h^2]^2}{16 M_P^2 E_h^2 m_\phi^2 E_h^4} = 0, \quad (\text{A.39})$$

for the same reason that Eq. (A.24) vanishes.

B Collision Terms Γ_h

In this section, we present in great detail the computation of the collision terms for the graviton production for the processes $\phi \rightarrow \varphi\varphi h$ and $\phi\phi \rightarrow \varphi h$, which are substantially more involved than $\phi\phi \rightarrow hh$ and $\varphi\varphi \rightarrow hh$.

B.1 $\phi \rightarrow \varphi\varphi h$

Labeling the particles in $\phi \rightarrow \varphi\varphi h$ from the left to the right by numbers 1 to 4 (with $E_4 = E_h$), Γ_h is then given by

$$\begin{aligned} \Gamma_h &= \frac{1}{2E_h} \int d\Pi_1 d\Pi_2 d\Pi_3 f_1 \frac{|\mathcal{M}_{\phi\rightarrow\varphi\varphi h}|^2}{2} (2\pi)^4 \delta^{(4)}(p_1 - p_2 - p_3 - p_4) \\ &= \frac{|\mathcal{M}_{\phi\rightarrow\varphi\varphi h}|^2}{2E_h} \int d\Pi_1 d\Pi_2 f_1 \frac{1}{2E_3} 2\pi \delta(E_1 - E_2 - E_3 - E_h), \end{aligned} \quad (\text{B.1})$$

where $E_3 = \sqrt{E_2 + E_4 + 2c_{24} E_2 E_h}$ with $c_{24} \equiv \vec{p}_2 \cdot \vec{p}_4 / (E_2 E_h)$ being the cosine of the angle between \vec{p}_2 and \vec{p}_4 , and noticing that $|\mathcal{M}_{\phi\rightarrow\varphi\varphi h}|^2$ can be moved outside the phase-space integral since it depends only on E_h ; cf Eq. (4.14). To integrate out the delta function, we should view it as a function of E_2 , E_h , and c_{24} :

$$\delta(E_1 - E_2 - E_3 - E_h) = \delta[F(E_2, E_h, c_{24})] \quad (\text{B.2})$$

with $F(E_2, E_h, c_{24}) = E_1 - E_2 - E_h - \sqrt{E_2^2 + E_h^2 + 2c_{24} E_2 E_h}$. It is straightforward to check that F as a function of c_{24} only has one root within $c_{24} \in [-1, 1]$, if and only if E_h and E_2 are in a triangle bounded by

$$E_h < \frac{m_\phi}{2}, \quad E_2 < \frac{m_\phi}{2}, \quad E_2 + E_h > \frac{m_\phi}{2}. \quad (\text{B.3})$$

With this triangle, we integrate out the delta function with c_{24} and then integrate E_2 from $m_\phi/2 - E_h$ to $m_\phi/2$, arriving at

$$\Gamma_h = \frac{|\mathcal{M}_{\phi \rightarrow \varphi \varphi h}|^2}{64\pi} \frac{n_\phi}{m_\phi p_h}. \quad (\text{B.4})$$

B.2 $\phi \varphi \rightarrow \varphi h$

The calculation of the collision term for $\phi \varphi \rightarrow \varphi h$ is similar to the calculation for $\phi \rightarrow \varphi \varphi h$ in the previous subsection; however, there are some differences. First, Eq. (B.1) is changed to

$$\begin{aligned} \Gamma_h &= \frac{1}{2E_h} \int d\Pi_1 d\Pi_2 d\Pi_3 f_1 f_2 |\mathcal{M}_{\phi \varphi \rightarrow \varphi h}|^2 (2\pi)^4 \delta^{(4)}(p_1 + p_2 - p_3 - p_4) \\ &= \frac{|\mathcal{M}_{\phi \varphi \rightarrow \varphi h}|^2}{2E_h} \int d\Pi_1 d\Pi_2 f_1 f_2 \frac{1}{2E_3} 2\pi \delta(E_1 + E_2 - E_3 - E_h). \end{aligned} \quad (\text{B.5})$$

Following a similar analysis on the delta function, we find that the triangle region bounded by Eq. (B.3) is changed to a region constrained by

$$\frac{m_\phi}{2} < E_h, \quad E_h - E_2 < \frac{m_\phi}{2}, \quad (\text{B.6})$$

which for $E_2 < \frac{m_\phi}{2}$ would imply that $E_h < m_\phi$, as already mentioned above. Then by integrating out c_{24} , we obtain

$$\Gamma_h = \frac{|\mathcal{M}_{\phi \varphi \rightarrow \varphi h}|^2 n_\phi}{32\pi m_\phi E_h^2} \int_{p_\varphi^{\min}}^{p_\varphi^{\max}} f_\varphi dp_\varphi, \quad (\text{B.7})$$

where $p_\varphi^{\min} \equiv E_h - \frac{m_\phi}{2}$ and $p_\varphi^{\max} = \frac{m_\phi}{2}$. Here, $p_\varphi^{\max} = \frac{m_\phi}{2}$ is imposed because f_φ has a cut-off point at $\frac{m_\phi}{2}$. If f_φ is a thermal distribution, then $p_\varphi^{\max} = \infty$ should be used. After substituting Eq. (3.15) into Eq. (B.7), the integration can be performed numerically. Analytically, we find that the result can be approximated by

$$\Gamma_h \simeq \frac{\pi}{2} \frac{\mu^2 n_\phi n_\varphi}{M_P^2 E_h^2 m_\phi^3} \left(1 - \frac{m_\phi}{2E_h}\right)^2 \tilde{\Theta} \left[\frac{1}{2} < \frac{E_h}{m_\phi} < 1 \right]. \quad (\text{B.8})$$

C Comparing Analytical with Numerical Results

In this section, we first offer some detailed steps for deriving the analytical expression for the gravitational spectra shown in the main text. Then, we compare them with the fully numerical results. The GW spectrum at present is

$$\begin{aligned} \Omega_{\text{GW}}(a_0) &= \frac{1}{\rho_c} f_h[a_0, p_h(a_0)] \frac{p_h^4(a_0)}{\pi^2} = \Omega_{\text{GW}}(a_\phi) \left(\frac{a_\phi}{a_0}\right)^4 \\ &= \frac{1}{\rho_c} f_h[a_\phi, p_h(a_\phi)] \frac{p_h^4(a_\phi)}{\pi^2} \left(\frac{a_\phi}{a_0}\right)^4. \end{aligned} \quad (\text{C.1})$$

We start by presenting the main channel in this work, namely $\phi\phi \rightarrow \varphi h$, where the phase-space distribution function at a_ϕ is given by Eq. (4.20). The corresponding GW spectrum is

$$\begin{aligned}\Omega_{\text{GW}}^{\phi\phi \rightarrow \varphi h}(f) &= \frac{1}{\rho_c} \frac{\pi}{4} \frac{M_P^2 \mu^2 H_I^2 \Gamma_\phi}{m_\phi^4} \left(\frac{a_I}{a_\phi}\right)^3 \frac{2\pi f a_0/a_\phi}{\pi^2} \left(\frac{a_\phi}{a_0}\right)^4 = \frac{1}{\rho_c} \frac{1}{2} \frac{M_P^2 \mu^2 H_I^2 \Gamma_\phi}{m_\phi^4} \left(\frac{a_I}{a_0}\right)^3 f \\ &\simeq \frac{1}{\rho_c} \frac{1}{2} \frac{M_P^2 \mu^2 H_I^2 \Gamma_\phi}{m_\phi^4} \left(\frac{2\Gamma_\phi}{3H_I}\right)^2 \left[\frac{\rho_{\text{SM}}(a_0)}{\frac{4}{3}\Gamma_\phi^2 M_P^2}\right]^{3/4} f \\ &\simeq 1.29 \times 10^{-15} \left(\frac{\mu}{10^{12} \text{ GeV}}\right)^5 \left(\frac{10^{13} \text{ GeV}}{m_\phi}\right)^{11/2} \left(\frac{f}{10^7 \text{ Hz}}\right).\end{aligned}\quad (\text{C.2})$$

We recall that the term H_I^2 in the first line of Eq. (C.2) originates from the number density n_ϕ in the initial state of the scattering process under consideration. A larger H_I implies that GW production occurs earlier, leading to a greater redshift for the produced gravitons. As seen in the last second step, the contribution from the inflationary scale H_I ultimately cancels out due to this redshift effect. Consequently, the maximal amplitude for the GW spectrum remains independent of H_I .

For the Bremsstrahlung channel $\phi \rightarrow \varphi \varphi h$, the phase-space distribution function at a_ϕ is given by Eq. (4.16), and the corresponding GW spectrum is

$$\begin{aligned}\Omega_{\text{GW}}^{\phi \rightarrow \varphi \varphi h}(f) &\simeq \frac{1}{\rho_c} \frac{1}{64\pi} \frac{\mu^2 H_I}{p_h^3(a_\phi)} \left(\frac{a_I}{a_\phi}\right)^{\frac{3}{2}} \frac{p_h^4(a_\phi)}{\pi^2} \left(\frac{a_\phi}{a_0}\right)^4 \\ &= \frac{1}{\rho_c} \frac{\mu^2 H_I}{64\pi} \left(\frac{a_I}{a_\phi}\right)^{\frac{3}{2}} \frac{2\pi f a_0/a_\phi}{\pi^2} \left(\frac{a_\phi}{a_0}\right)^4 \\ &\simeq 2.15 \times 10^{-20} \left(\frac{\mu}{10^{12} \text{ GeV}}\right) \left(\frac{m_\phi}{10^{13} \text{ GeV}}\right)^{1/2} \left(\frac{f}{10^7 \text{ Hz}}\right).\end{aligned}\quad (\text{C.3})$$

Similarly to the previous case, the dependence of H_I cancels out, leading to a maximal amplitude for the spectrum independent of it.

For $\phi\phi \rightarrow hh$, the phase-space distribution function at a_ϕ given in Eq. (4.8) generates a GW spectrum

$$\begin{aligned}\Omega_{\text{GW}}^{\phi\phi \rightarrow hh}(f) &\simeq \frac{1}{\rho_c} \frac{9\pi m_\phi^{\frac{3}{2}} H_I^3}{16} \frac{1}{p_h^{\frac{9}{2}}(a_\phi)} \left(\frac{a_I}{a_\phi}\right)^{\frac{9}{2}} \frac{p_h^4(a_\phi)}{\pi^2} \left(\frac{a_\phi}{a_0}\right)^4 \\ &\simeq \frac{1}{\rho_c} \frac{9 m_\phi^{\frac{3}{2}} H_I^3}{16\pi} \frac{1}{(2\pi f a_0/a_\phi)^{\frac{1}{2}}} \left(\frac{a_I}{a_\phi}\right)^{\frac{9}{2}} \left(\frac{a_\phi}{a_0}\right)^4 \simeq \frac{1}{\rho_c} \frac{9 m_\phi^{\frac{3}{2}} H_I^3}{16\pi} \frac{1}{(2\pi f)^{\frac{1}{2}}} \left(\frac{a_I}{a_0}\right)^{\frac{9}{2}} \\ &\simeq 1.25 \times 10^{-19} \left(\frac{\mu}{10^{12} \text{ GeV}}\right)^{\frac{3}{2}} \left(\frac{m_\phi}{10^{13} \text{ GeV}}\right)^{\frac{3}{4}} \left(\frac{f}{10^7 \text{ Hz}}\right)^{-\frac{1}{2}}.\end{aligned}\quad (\text{C.4})$$

Finally, for $\varphi\varphi \rightarrow hh$, the phase-space distribution function at a_ϕ is given by Eq. (4.25),

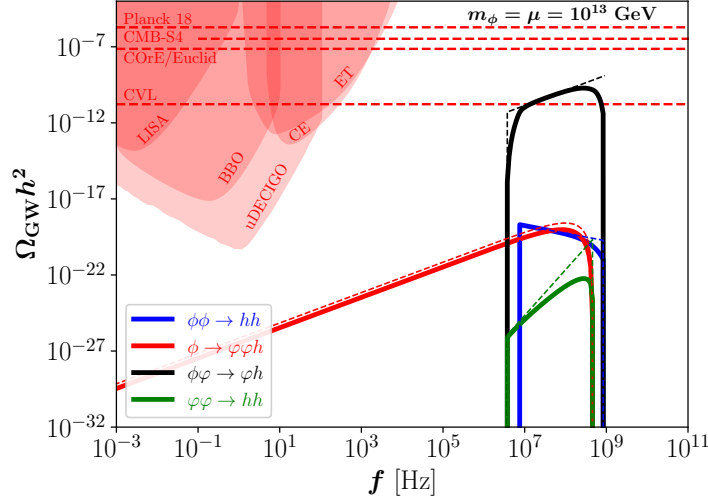


Figure 5. Comparison of the fully numerical spectra (thick solid lines) and the analytical approximations (thin dashed lines), for $m_\phi = \mu = 10^{13}$ GeV and $H_I = 2.0 \times 10^{-5} M_P$.

and the corresponding GW spectrum is

$$\begin{aligned}
 \Omega_{\text{GW}}^{\phi\phi \rightarrow hh} &\simeq \frac{1}{\rho_c} \frac{9\pi H_I \Gamma^2}{140 m_\phi^2 p_h(a_\phi)} \frac{a_I p_h^4(a_\phi)}{a_\phi \pi^2} \left(\frac{a_\phi}{a_0}\right)^4 \\
 &= \frac{1}{\rho_c} \frac{9 H_I \Gamma^2 \pi [2\pi f a_0/a_\phi]^3}{140 m_\phi^2 \pi^2} \frac{a_I}{a_\phi} \left(\frac{a_\phi}{a_0}\right)^4 = \frac{1}{\rho_c} \frac{18 H_I \Gamma^2 \pi^2}{35 m_\phi^2} \left(\frac{a_I}{a_0}\right) f^3 \\
 &\simeq 2.9 \times 10^{-29} \left(\frac{H_I}{2.0 \times 10^{-5} M_P}\right)^{\frac{1}{3}} \left(\frac{\mu}{10^{12} \text{ GeV}}\right)^{\frac{13}{3}} \left(\frac{10^{13} \text{ GeV}}{m_\phi}\right)^{\frac{25}{6}} \left(\frac{f}{10^7 \text{ Hz}}\right)^3.
 \end{aligned} \tag{C.5}$$

Figure 5 presents a comparison between the fully numerical computation of GW spectra (thick solid lines) and the corresponding approximate analytical expressions (thin dashed lines) for $m_\phi = \mu = 10^{13}$ GeV and $H_I = 2.0 \times 10^{-5} M_P$. Very good agreement is found.

References

- [1] C. Caprini and D.G. Figueroa, *Cosmological Backgrounds of Gravitational Waves*, *Class. Quant. Grav.* **35** (2018) 163001 [[1801.04268](#)].
- [2] M. Kawasaki, K. Kohri and N. Sugiyama, *MeV scale reheating temperature and thermalization of neutrino background*, *Phys. Rev. D* **62** (2000) 023506 [[astro-ph/0002127](#)].
- [3] S. Hannestad, *What is the lowest possible reheating temperature?*, *Phys. Rev. D* **70** (2004) 043506 [[astro-ph/0403291](#)].
- [4] R.H. Cyburt, B.D. Fields, K.A. Olive and T.-H. Yeh, *Big Bang Nucleosynthesis: 2015*, *Rev. Mod. Phys.* **88** (2016) 015004 [[1505.01076](#)].
- [5] P.F. de Salas, M. Lattanzi, G. Mangano, G. Miele, S. Pastor and O. Pisanti, *Bounds on very low reheating scenarios after Planck*, *Phys. Rev. D* **92** (2015) 123534 [[1511.00672](#)].

- [6] R. Allahverdi, R. Brandenberger, F.-Y. Cyr-Racine and A. Mazumdar, *Reheating in Inflationary Cosmology: Theory and Applications*, *Ann. Rev. Nucl. Part. Sci.* **60** (2010) 27 [[1001.2600](#)].
- [7] M.A. Amin, M.P. Hertzberg, D.I. Kaiser and J. Karouby, *Nonperturbative Dynamics Of Reheating After Inflation: A Review*, *Int. J. Mod. Phys. D* **24** (2014) 1530003 [[1410.3808](#)].
- [8] K.D. Lozanov, *Lectures on Reheating after Inflation*, [1907.04402](#).
- [9] K. Nakayama and Y. Tang, *Stochastic Gravitational Waves from Particle Origin*, *Phys. Lett. B* **788** (2019) 341 [[1810.04975](#)].
- [10] D. Huang and L. Yin, *Stochastic Gravitational Waves from Inflaton Decays*, *Phys. Rev. D* **100** (2019) 043538 [[1905.08510](#)].
- [11] B. Barman, N. Bernal, Y. Xu and Ó. Zapata, *Gravitational wave from graviton Bremsstrahlung during reheating*, *JCAP* **05** (2023) 019 [[2301.11345](#)].
- [12] B. Barman, N. Bernal, Y. Xu and Ó. Zapata, *Bremsstrahlung-induced gravitational waves in monomial potentials during reheating*, *Phys. Rev. D* **108** (2023) 083524 [[2305.16388](#)].
- [13] S. Kanemura and K. Kaneta, *Gravitational waves from particle decays during reheating*, *Phys. Lett. B* **855** (2024) 138807 [[2310.12023](#)].
- [14] N. Bernal, S. Cléry, Y. Mambrini and Y. Xu, *Probing reheating with graviton bremsstrahlung*, *JCAP* **01** (2024) 065 [[2311.12694](#)].
- [15] A. Tokareva, *Gravitational waves from inflaton decay and bremsstrahlung*, *Phys. Lett. B* **853** (2024) 138695 [[2312.16691](#)].
- [16] W. Hu, K. Nakayama, V. Takhistov and Y. Tang, *Gravitational wave probe of Planck-scale physics after inflation*, *Phys. Lett. B* **856** (2024) 138958 [[2403.13882](#)].
- [17] K.-Y. Choi, E. Lkhagvadorj and S. Mahapatra, *Gravitational wave sourced by decay of massive particle from primordial black hole evaporation*, *JCAP* **07** (2024) 064 [[2403.15269](#)].
- [18] B. Barman, N. Bernal, S. Cléry, Y. Mambrini, Y. Xu and Ó. Zapata, *Probing Reheating with Gravitational Waves from Graviton Bremsstrahlung*, in *58th Rencontres de Moriond on Electroweak Interactions and Unified Theories*, 5, 2024 [[2405.09620](#)].
- [19] R. Inui, Y. Mikura and S. Yokoyama, *Gravitational waves from graviton bremsstrahlung with kination phase*, *Phys. Rev. D* **111** (2025) 043511 [[2408.10786](#)].
- [20] Y. Jiang and T. Suyama, *Spectrum of high-frequency gravitational waves from graviton bremsstrahlung by the decay of inflaton: case with polynomial potential*, [2410.11175](#).
- [21] Y. Ema, R. Jinno, K. Mukaida and K. Nakayama, *Gravitational Effects on Inflaton Decay*, *JCAP* **05** (2015) 038 [[1502.02475](#)].
- [22] Y. Ema, R. Jinno, K. Mukaida and K. Nakayama, *Gravitational particle production in oscillating backgrounds and its cosmological implications*, *Phys. Rev. D* **94** (2016) 063517 [[1604.08898](#)].
- [23] Y. Ema, R. Jinno and K. Nakayama, *High-frequency Graviton from Inflaton Oscillation*, *JCAP* **09** (2020) 015 [[2006.09972](#)].
- [24] G. Choi, W. Ke and K.A. Olive, *Minimal production of prompt gravitational waves during reheating*, *Phys. Rev. D* **109** (2024) 083516 [[2402.04310](#)].

- [25] Y. Xu, *Ultra-high frequency gravitational waves from scattering, Bremsstrahlung and decay during reheating*, *JHEP* **10** (2024) 174 [[2407.03256](#)].
- [26] N. Bernal and Y. Xu, *Thermal gravitational waves during reheating*, *JHEP* **01** (2025) 137 [[2410.21385](#)].
- [27] J. Ghiglieri and M. Laine, *Gravitational wave background from Standard Model physics: Qualitative features*, *JCAP* **07** (2015) 022 [[1504.02569](#)].
- [28] J. Ghiglieri, G. Jackson, M. Laine and Y. Zhu, *Gravitational wave background from Standard Model physics: Complete leading order*, *JHEP* **07** (2020) 092 [[2004.11392](#)].
- [29] A. Ringwald, J. Schütte-Engel and C. Tamarit, *Gravitational Waves as a Big Bang Thermometer*, *JCAP* **03** (2021) 054 [[2011.04731](#)].
- [30] P. Klose, M. Laine and S. Procacci, *Gravitational wave background from non-Abelian reheating after axion-like inflation*, *JCAP* **05** (2022) 021 [[2201.02317](#)].
- [31] A. Ringwald and C. Tamarit, *Revealing the cosmic history with gravitational waves*, *Phys. Rev. D* **106** (2022) 063027 [[2203.00621](#)].
- [32] P. Klose, M. Laine and S. Procacci, *Gravitational wave background from vacuum and thermal fluctuations during axion-like inflation*, *JCAP* **12** (2022) 020 [[2210.11710](#)].
- [33] J. Ghiglieri, J. Schütte-Engel and E. Speranza, *Freezing-in gravitational waves*, *Phys. Rev. D* **109** (2024) 023538 [[2211.16513](#)].
- [34] M. Drewes, Y. Georis, J. Klaric and P. Klose, *Upper bound on thermal gravitational wave backgrounds from hidden sectors*, *JCAP* **06** (2024) 073 [[2312.13855](#)].
- [35] J. Ghiglieri, M. Laine, J. Schütte-Engel and E. Speranza, *Double-graviton production from Standard Model plasma*, *JCAP* **04** (2024) 062 [[2401.08766](#)].
- [36] M.A.G. García and M.A. Amin, *Prethermalization production of dark matter*, *Phys. Rev. D* **98** (2018) 103504 [[1806.01865](#)].
- [37] C.W. Misner, K.S. Thorne and J.A. Wheeler, *Gravitation*, W. H. Freeman, San Francisco (1973).
- [38] J.F. Donoghue, *General relativity as an effective field theory: The leading quantum corrections*, *Phys. Rev. D* **50** (1994) 3874 [[gr-qc/9405057](#)].
- [39] S.Y. Choi, J.S. Shim and H.S. Song, *Factorization and polarization in linearized gravity*, *Phys. Rev. D* **51** (1995) 2751 [[hep-th/9411092](#)].
- [40] A.A. Starobinsky, *A New Type of Isotropic Cosmological Models Without Singularity*, *Phys. Lett. B* **91** (1980) 99.
- [41] R. Kallosh and A. Linde, *Universality Class in Conformal Inflation*, *JCAP* **07** (2013) 002 [[1306.5220](#)].
- [42] R. Kallosh and A. Linde, *Non-minimal Inflationary Attractors*, *JCAP* **10** (2013) 033 [[1307.7938](#)].
- [43] M. Drees and Y. Xu, *Small field polynomial inflation: reheating, radiative stability and lower bound*, *JCAP* **09** (2021) 012 [[2104.03977](#)].
- [44] N. Bernal and Y. Xu, *Polynomial inflation and dark matter*, *Eur. Phys. J. C* **81** (2021) 877 [[2106.03950](#)].

- [45] M. Drees and Y. Xu, *Large field polynomial inflation: parameter space, predictions and (double) eternal nature*, *JCAP* **12** (2022) 005 [[2209.07545](#)].
- [46] N. Bernal, J. Harz, M.A. Mojahed and Y. Xu, *Graviton- and inflaton-mediated dark matter production after large field polynomial inflation*, *Phys. Rev. D* **111** (2025) 043517 [[2406.19447](#)].
- [47] Q.-f. Wu and X.-J. Xu, *High-energy and ultra-high-energy neutrinos from Primordial Black Holes*, *JCAP* **02** (2025) 059 [[2409.09468](#)].
- [48] BICEP, KECK collaboration, *Improved Constraints on Primordial Gravitational Waves using Planck, WMAP, and BICEP/Keck Observations through the 2018 Observing Season*, *Phys. Rev. Lett.* **127** (2021) 151301 [[2110.00483](#)].
- [49] T. Hasegawa, N. Hiroshima, K. Kohri, R.S.L. Hansen, T. Tram and S. Hannestad, *MeV-scale reheating temperature and thermalization of oscillating neutrinos by radiative and hadronic decays of massive particles*, *JCAP* **12** (2019) 012 [[1908.10189](#)].
- [50] PARTICLE DATA GROUP collaboration, *Review of particle physics*, *Phys. Rev. D* **110** (2024) 030001.
- [51] LISA collaboration, *Laser Interferometer Space Antenna*, [1702.00786](#).
- [52] M. Punturo et al., *The Einstein Telescope: A third-generation gravitational wave observatory*, *Class. Quant. Grav.* **27** (2010) 194002.
- [53] S. Hild et al., *Sensitivity Studies for Third-Generation Gravitational Wave Observatories*, *Class. Quant. Grav.* **28** (2011) 094013 [[1012.0908](#)].
- [54] B. Sathyaprakash et al., *Scientific Objectives of Einstein Telescope*, *Class. Quant. Grav.* **29** (2012) 124013 [[1206.0331](#)].
- [55] ET collaboration, *Science Case for the Einstein Telescope*, *JCAP* **03** (2020) 050 [[1912.02622](#)].
- [56] D. Reitze et al., *Cosmic Explorer: The U.S. Contribution to Gravitational-Wave Astronomy beyond LIGO*, *Bull. Am. Astron. Soc.* **51** (2019) 035 [[1907.04833](#)].
- [57] J. Crowder and N.J. Cornish, *Beyond LISA: Exploring future gravitational wave missions*, *Phys. Rev. D* **72** (2005) 083005 [[gr-qc/0506015](#)].
- [58] V. Corbin and N.J. Cornish, *Detecting the cosmic gravitational wave background with the big bang observer*, *Class. Quant. Grav.* **23** (2006) 2435 [[gr-qc/0512039](#)].
- [59] G.M. Harry, P. Fritschel, D.A. Shaddock, W. Folkner and E.S. Phinney, *Laser interferometry for the big bang observer*, *Class. Quant. Grav.* **23** (2006) 4887.
- [60] N. Seto, S. Kawamura and T. Nakamura, *Possibility of direct measurement of the acceleration of the universe using 0.1-Hz band laser interferometer gravitational wave antenna in space*, *Phys. Rev. Lett.* **87** (2001) 221103 [[astro-ph/0108011](#)].
- [61] H. Kudoh, A. Taruya, T. Hiramatsu and Y. Himemoto, *Detecting a gravitational-wave background with next-generation space interferometers*, *Phys. Rev. D* **73** (2006) 064006 [[gr-qc/0511145](#)].
- [62] PLANCK collaboration, *Planck 2018 results. VI. Cosmological parameters*, *Astron. Astrophys.* **641** (2020) A6 [[1807.06209](#)].
- [63] CORE collaboration, *COrE (Cosmic Origins Explorer) A White Paper*, [1102.2181](#).

- [64] EUCLID collaboration, *Euclid Definition Study Report*, [1110.3193](#).
- [65] K. Abazajian et al., *CMB-S4 Science Case, Reference Design, and Project Plan*, [1907.04473](#).
- [66] I. Ben-Dayan, B. Keating, D. Leon and I. Wolfson, *Constraints on scalar and tensor spectra from N_{eff}* , *JCAP* **06** (2019) 007 [[1903.11843](#)].